


## RESEARCH ARTICLE OPEN ACCESS

# Predicting and Controlling Multiple Transmissions of Rotavirus Using Computational Biomedical Model in Smart Health Infrastructures

Titus Ifeanyi Chinebu<sup>1</sup> | Kennedy Chinedu Okafor<sup>2,3,4,5</sup>  | Omowunmi Mary Longe<sup>4</sup> | Kelvin Anoh<sup>5</sup> | Henrietta Onyinye Uzoeto<sup>1</sup> | Victor Onukwube Apeh<sup>1</sup> | Ijeoma Peace Okafor<sup>6</sup> | Bamidele Adebisi<sup>3</sup> | Chukwunenye Anthony Okoronkwo<sup>2</sup>

<sup>1</sup>Department of Applied Sciences, Federal University of Allied Health Sciences, Enugu, Nigeria | <sup>2</sup>Department of Mechatronics Engineering, Federal University of Technology, Owerri, Nigeria | <sup>3</sup>Department of Engineering, Manchester Metropolitan University, Manchester, UK | <sup>4</sup>Department of Electrical and Electronic Engineering Science, University of Johannesburg, Johannesburg, South Africa | <sup>5</sup>Center For Future Technologies, University of Chichester, Bognor Regis, UK | <sup>6</sup>Department of Public Health, Cardiff Metropolitan University, Llandaff Campus, Cardiff, UK

**Correspondence:** Kennedy Chinedu Okafor ([kennedy.okafor@mmu.ac.uk](mailto:kennedy.okafor@mmu.ac.uk))

**Received:** 25 September 2024 | **Revised:** 19 December 2024 | **Accepted:** 27 March 2025

**Funding:** This research is partly sponsored by the Nigeria Tertiary Education Fund, TETFUND under the grant number TETF/ES/UNIV/IMO STATE/TSAS/2021.

**Keywords:** applied mathematics | computational biomedical model | electron microscopy | internet of things | Lyapunov function | smart health infrastructure

## ABSTRACT

Conventional laboratory investigation of rotavirus infection and its antigen in rectal swabs from infected persons uses Electron microscopy (EM) (i.e., non-acute cases), genome, and antigen-detecting assays. A recent update involves sorting, trapping, concentrating, and identifying infectious rotavirus particles in clinical samples leveraging activated magnetic microparticles with monoclonal antibodies. However, the routine detection of rotavirus in many specimens using the EM approach is laborious, costly, and requires highly skilled workers. A sustainable healthcare system should leverage the Internet of Things to operate Smart Health Infrastructures (SHI) for predictive control of contagious diseases such as the rotavirus. This paper proposes a biomedical model for predictive control of the virus spread based on Susceptible, Breastfeeding, Vaccinated, Infected, and Recovered (SBVIR) parameters. We introduce breastfeeding, vaccination, and saturated incidence rate variables to deconstruct the transmission dynamics. An efficiency test is conducted using RI control parameters  $B$  and  $V$ . Applying Lyapunov function analysis, we prove that the global stability of disease-free and endemic equilibria exists under breastfeeding and vaccination conditions when the primary reproduction number is less than unity. Numerical simulation results show that breastfeeding and vaccination are optimal with SBVIR compared to SVIR, SBIR, and SIR parameters for rotavirus infection control by 99%, 26%, 19%, and 18%, respectively. On top of these, we show that the SBVIR model strongly agrees with real-world data and can be used to forecast the infected population in a production health facility. Finally, we show multiple Internet of Things applications in SHI to control rotavirus transmission effectively.

This is an open access article under the terms of the [Creative Commons Attribution](https://creativecommons.org/licenses/by/4.0/) License, which permits use, distribution and reproduction in any medium, provided the original work is properly cited.

© 2025 The Author(s). *Engineering Reports* published by John Wiley & Sons, Ltd.

## 1 | Introduction

Despite the widespread implementation of interventions aimed at revolutionizing the provision of health and social care, rotaviruses persist as a primary and pervasive cause of diarrhea among newborns and young children [1, 2]. In context, the oral–fecal pathway is the vector channel for the virus's spread [3]. This causes gastroenteritis, sometimes known as the “stomach flu” by infecting and destroying the cells lining the small intestine in tropical countries, particularly South-east, and Southern Asia, including Africa [2]. The traditional method for diagnosing rotavirus involves Electron microscopy, genome, and antigen detection tests [2]. Given its complex molecular epidemiology, infants in hospitals and young children in daycare facilities frequently exhibit the symptoms of diarrhea caused by the infection. Most care homes and rural hospitals still suffer from the spread of various similar communicable diseases [1].

The World Health Organization (WHO) estimates that rotavirus infection killed about 580,000 people worldwide in 2004 [3], and this is largely in underdeveloped countries. It was estimated that rotavirus diarrhea was responsible for 47,898 deaths annually in under-five children in Nigeria [4]. Infection is the leading cause of severe diarrheal illness in newborns and young children. While many viral strains exist, five serotypes are responsible for most human rotavirus infections [5]. Rotaviruses typically infect most children worldwide before the age of three, and in many underdeveloped nations, before their first birthday. With each infection, immunity increases, making subsequent infections less severe; as a result, adults are rarely affected [6]. Rotavirus can enter the human body through the fecal-oral route via contaminated hands, environmental surfaces, and objects, and occasionally through food and water [6]. Human rotavirus infections can cause a range of clinical symptoms, from mild illness with minor diarrhea to severe, recurring diarrhea accompanied by high fever and vomiting. This can lead to dehydration, electrolyte imbalance, and, in severe cases, death [6].

Rotavirus infection often begins with a severe episode of vomiting and fever lasting 3 to 7 days [7]. Vaccination can aid in prevention, although it is not effective during the first 2 months [8], while breastfeeding is believed to provide additional preventive benefits [9]. The authors in [10] investigated the benefits, limits, and potential development of artificial intelligence on prediction models used to study gastroenterology infection. Recognizing that breastfeeding may reduce gastrointestinal infections due to breast lymphocytes, the researchers in [11] carried out sentiment analysis using lexicon-based machine learning techniques. In another study, breastfeeding is identified as helping to reduce gastrointestinal infections [12]. This is because breast milk contains lymphocytes, bactericidal lactoferrin, and oligosaccharides. Additionally, breast milk is rich in immunoglobulins, which protect infants from diseases like pneumonia, diarrhea, ear infections, and asthma. It offers immediate defense against rotavirus infection and aids in immunological activation [11]. Breastfed infants tend to experience fewer acute illnesses, such as diarrhea, which decreases morbidity and mortality from diarrheal diseases during childhood [13, 14].

To enhance protection against rotavirus, the government of Nigeria, through the National Primary Health Care Development Agency (NPHCDA), with support from the WHO and partners, introduced the rotavirus vaccine into the Routine Immunization (RI) Schedule on August 22, 2022. This initiative aims to address the significant burden of rotavirus-related diarrheal disease and is expected to prevent over 50,000 child deaths annually. The vaccine is provided free of charge to all infants at the ages of 6, 10, and 14 weeks, alongside other vaccines included in the RI program, and is available at healthcare facilities across the country [15].

A robust solution to further control the spread of rotavirus and other contagious diseases could be achieved by leveraging a sustainable healthcare system that incorporates advanced technologies. By utilizing the Internet of Things (IoT) to operate Smart Health Infrastructures (SHI), predictive control of disease outbreaks can be significantly enhanced. This paper proposes a biomedical model for the predictive control of rotavirus spread based on Susceptible, Breastfeeding, Vaccinated, Infected, and Recovered (SBVIR) parameters. Our model introduces variables for breastfeeding, vaccination, and a saturated incidence rate to thoroughly analyze and deconstruct the transmission dynamics of the virus. This approach aims to improve the prediction and management of disease outbreaks through advanced technological integration and data-driven strategies.

To the best knowledge of the authors, this paper offers a novel perspective on health informatics while addressing its limitations and outlining potential future implementations. The main contributions of this study include:

- developed a Biomedical model that captures the dynamics of rotavirus infection for both symptomatic and asymptomatic individuals;
- identified and designed epidemiologically and biologically feasible regions within the infection dynamics model;
- derived models for disease equilibrium and stability to better understand the conditions under which the disease can be controlled or eradicated;
- formulated a differential equation that incorporates breastfeeding and vaccination to model saturation incidence rates for rotavirus;
- validated the model by comparing scenarios with controlled and uncontrolled saturation incidence rates, assessing the effectiveness of breastfeeding and vaccination in controlling the spread of the infection;
- demonstration of multiple IoT applications in SHI to control rotavirus transmission effectively.

The remaining parts of this study are organized as follows. Section 2 highlights brief literature and gaps. Section 3 discusses the main system assumptions and main methods. Section 4 presents the primary theory, while Section 5 presents the results. Research discussions are presented in Section 6 and Section 7 concludes the paper with future directions.

## 2 | Related Works

In this subsection, we discuss related efforts. In [16], the authors used mathematical models to investigate variations in rotavirus incidence among children under five in Ghana, fitting the models with case-control and surveillance data from three hospitals. In [17], the authors demonstrated that vaccination is a successful intervention against severe rotavirus-associated gastroenteritis (RVGE) in sub-Saharan Africa. While the rotavirus vaccine shows high effectiveness (85%–99%) in high-income countries (HICs), its effectiveness is generally lower (50%–64%) in low-income countries (LICs). In [18], researchers proposed agent-based computational modeling to evaluate oncolytic viral effectiveness. Works [19–21] used computational models to assess virus matrix assembly kinetics.

In [22], the study examined the Atangana-Baleanu derivative-based fractional-order model of the rotavirus epidemic, incorporating the effects of nursing and vaccination. The researchers applied Krasnoselskii and Banach fixed-point theorems to establish the model's existence and uniqueness. In [23], the authors tested the stability of their vaccine using molecular dynamics simulations for rotavirus multi-threading models. Their computational models aimed to advance epitope-based vaccination and diagnostic tests for rotavirus-induced diarrhea in children.

Finally, [24] estimated the long-term effects of rotavirus vaccination on deaths and disability-adjusted life years across 112 low- and middle-income countries from 2006 to 2034 using a transmission model. This study also examined the relative contributions of direct and indirect effects and compared the efficacy of one- versus two-dose vaccine series. The authors suggest that infants should receive the rotavirus vaccine to enhance protection against the disease [25].

The primary goal of predicting and controlling multiple transmissions of rotavirus is to develop a suitable framework for addressing the communicable diseases during epidemics and pandemics. A model for controlling rotavirus disease has been presented in [26] using breastfeeding and vaccination as the control variables in the presence of Susceptible  $S(t)$ , Breastfeeding  $B(t)$ , Infected  $I(t)$ , and Recovered  $R(t)$  populations; this is the well-known SBIR-Model. That study could not account for the saturated incidence rate that describes the rate at which new infections change with the increasing number of susceptible, breastfeeding and vaccinated individuals. It becomes particularly relevant in situations where the transmission rate does not increase indefinitely with more susceptible individuals due to limitations such as behavioral changes, resource constraints, or other factors that prevent an infinite rise in new infections. By incorporating these saturated incidence rates, the model will more accurately reflect how rotavirus spreads in a population with varying levels of susceptibility, breastfeeding, and vaccination. It acknowledges that interventions have limits and that transmission dynamics are not always linear. Understanding these saturation points allows public health officials to make more informed decisions about how to allocate resources, prioritize interventions, and set achievable goals for controlling rotavirus infections. It prevents overestimations of the impact of increasing breastfeeding or vaccination rates beyond their saturation points.

The work [27, 28] introduced the saturated incidence rate  $\frac{\beta SI}{1+\alpha I}$  which tends to a saturated level when  $I$  gets large,  $\beta I$  measures the infection force when the disease enters a fully susceptible population, and  $\frac{1}{1+\alpha I}$  measures the inhibitory effect from the behavioral change of susceptible individuals when their number increases or forms the crowding effect of the infective individuals.

This saturated incidence rate was used in many epidemics and the rotavirus models [19, 24, 29]. This paper then established a biomedical computational model for studying the dynamics of Rotavirus infection (RI) with saturation incidence and control. Selected metrics used in the study population include saturation incidence, breastfeeding, and vaccination.

Several articles have examined the dynamics of rotavirus transmission and infection control using mathematical models. In [30], a new model for RI that integrates vaccination was developed which was thoroughly examined and demonstrated that an endemic equilibrium existed, (i.e.,  $E^* = (S^*, V^*, I^*)$ ). The authors [26] developed a RI model that considers immunization and saturation incidence. Their concept model was generalized considering the saturation incidence rate that occurs when diseased people come into touch with immunized people. Since rotavirus has a high shading rate among infected individuals, the environmental effect is often considered when analyzing its transmission dynamics. Therefore, the authors [31] involved both environmental-to-human and human-to-human transmission interactions in their model.

To examine breastfeeding on RI prevention, a model was developed to analyze the impact of  $B$  and  $V$  on rotavirus epidemics [26]. Similarly, the work [32] investigated how time-lapse impacts the effectiveness of the vaccine. It was observed that delays in receiving booster shots or vaccination doses can reduce immunity, raise the possibility of viral mutations, and lengthen the pandemic by delaying the establishment of broad immunity. This delay could impede efforts to stop the virus's transmission and result in more infections that emerge as breakthroughs and inadequate immunity.

The following gaps were identified from the existing works [10, 26, 32, 33]:

- i. There is a non-existent saturation incidence to shrink the dynamics of infection among individuals who lose their maternal antibody obtained through breastfeeding from the existing studies.
- ii. Limited works dealt with minimizing the infection due to the waning of vaccines using saturation incidence rate.
- iii. None of the existing models considered combining the reduction in the size of the infected population due to the loss of maternal antibodies from breastfeeding and the waning of vaccine immunity, using a saturation incidence rate.

## 3 | Materials and Methods

In mathematical epidemiology, data availability is often limited, and integrating subsystem models into a comprehensive model

is rarely straightforward. As a result, assumptions and estimates are necessary at nearly every stage of the process. In this paper, we clearly outline the assumptions and define the key nomenclature used throughout. A computational numerical approach is used to verify the results in Section 5.

### 3.1 | Model Assumptions

- The model demographic progression is through the recruitment of newborns or migration of children under 5 years in the population.
- All children under 5 years in the population are susceptible to rotavirus.
- Rotavirus infection can be controlled through vaccination and maternal antigen from breastfeeding.
- Both the maternal antibodies from breast milk and the vaccine may wane off since they are temporarily effective; however, the population should receive ongoing vaccinations steadily.
- Systems and equations are used interchangeably.

### 3.2 | Nomenclature

Table 1 provides the nomenclature, meanings, and parameter values for various components of the disease models, comparing scenarios with and without breastfeeding and vaccination, along with the sources of these values.

## 4 | Theory and System Modeling

We consider the population of kids less than 5 years, divided into five groups of susceptible ( $S(t)$ ), breastfeeding ( $B(t)$ ), vaccinated ( $V(t)$ ), infected ( $I(t)$ ) and recovered ( $R(t)$ ), all at time  $t$ . This can be denoted as the SBVIR model where  $S$  is the susceptible children (those who are vulnerable to rotavirus infection),  $B$  is the breastfeeding children (those who started breastfeeding immediately after birth),  $V$  is the vaccinated children (those who have received vaccines protection against rotavirus infection),  $I$  is infected (those who are already infected with rotavirus disease) and  $R$  is recovered (those who have recovered from the infection due to treatment). The total population is expressed as

$$N(t) = S(t) + B(t) + V(t) + I(t) + R(t) \quad (1)$$

The model in Equation (1) generally allows us to include a variety of population parameters relating to the rotavirus that impacts the population. Since birth, immigration, emigration, and death are non-constant factors, the population of children either rises or falls. In most cases, children can develop some level of immunity to rotavirus infection from maternal antibodies due to breastfeeding, but this immunity does not last for a long time [30], hence vaccination is necessary [14]. Rotavirus-infected children are both symptomatic and asymptomatic [40] and immunity develops with each infection, making subsequent infections less severe. Due to developed immunity, children who are removed from an infectious population do so in the recovered group.

Breastfed children can receive vaccinations because both  $B$  and  $V$  lower the risk of rotavirus infection. Figure 1 shows the movement from one group to another.

The admission into vulnerable-susceptible, breastfeeding, and vaccinated groups takes place at rates  $(1 - \rho - \alpha)\psi$ ,  $\rho\psi$ , and  $\alpha\psi$ , respectively. Susceptible children breastfeed at a rate  $\Lambda$  and the antibodies from maternal breast milk waneoff at  $\tau$ . Now the kids come back to the susceptible group. The vaccination rate of children in the breastfeeding group is denoted as  $\xi$ . Children in the susceptible group are vaccinated at a rate  $\omega$  and the waning rate of vaccine is denoted as  $\gamma$ . The transmission of rotavirus between the susceptible and infected group is  $\beta SI$  while  $\beta$  is the rotavirus transmission rate. The anticipated decline in the infection risk is because  $B$  and  $V$  are at a rate  $\epsilon$  and  $\eta$ , respectively, where  $\epsilon, \eta \in (0, 1)$ . In addition,  $\mu$  denotes the normal death trend of children and  $\phi$  represents the rotavirus-incited death rate of affected children. Infected children who become sick kids may recover at a rate  $\theta$ . We represent the saturation constant of incidence transmission of  $S$  and  $I$  as  $\sigma_1$ , the constant of saturation incidence of transmission of  $B$  and  $I$  represented as  $\sigma_2$  and the saturation incidence of transmission of  $V$  and  $I$  as  $\sigma_3$ .

### 4.1 | Model Formulation

To control the rate of rotavirus contraction, we need to develop a model for the spread of the virus as shown in (2). We start by considering a population of susceptible children. Our model uses a saturation incidence function,  $f(\sigma, \beta) = \frac{\beta I}{1 + \sigma I}$ . We assume that susceptible children enter the population at a rate of  $(1 - \rho - \alpha)$ , representing children born into the population at time  $t$ . These children are breastfed at a rate  $\Lambda$  and vaccinated at a rate  $\omega$ . Breastfeeding helps control the virus's spread, and we denote the rate at which breastfeeding protection wanes as  $\tau$ , while the vaccine's waning rate is  $\gamma$ . Susceptible children get infected at a rate of  $\frac{\beta SI}{1 + \sigma_1 I}$  and die naturally at a rate  $\mu$ . Therefore, the rate of susceptibility of children to the virus can be expressed as

$$\frac{dS(t)}{dt} = (1 - \rho - \alpha)\psi + \tau B + \gamma V - \left( \frac{\beta I}{1 + \sigma_1 I} + \Lambda + \omega + \mu \right) S \quad (2a)$$

To protect the population, we need to manage the rates at which children move between different compartments and face various risks. Let's discuss how the breastfeeding rate and related dynamics work:

- Newborn Children:** Newborn children in the susceptible group are breastfed at a rate  $\Lambda$ . As the maternal antibodies from breast milk wane at a rate  $\tau$ , these children eventually return to the susceptible compartment.
- Population Growth:**
  - The population of breastfed children increases by  $\rho\psi$  from already breastfed children entering the population.
  - The vaccinated population grows by  $\alpha\psi$
  - Susceptible children are vaccinated at a rate of  $\omega S$
- Decrease in Breastfed Population:**
  - The population of breastfed children decreases due to rotavirus infection at a rate of  $\frac{\epsilon \beta I}{1 + \sigma_2 I}$ .



**TABLE 1** | Basic nomenclature.

Nomenclature	Meaning	Parameter values with breastfeeding and vaccination	Parameter values without breastfeeding and vaccination	Source
SVIR	Susceptible, vaccinated, infected and recovered	—	—	—
SBIR	Susceptible, breastfeeding, infected, and recovered	—	—	—
SIR	Susceptible, infected, and recovered.	—	—	—
(S(t))	Susceptible children	2000	2000	[27]
(B(t))	Breastfeeding children	1500	1500	[27]
(V(t))	Vaccinated children	1500	1500	[27]
I(t)	Infected children	100	100	[27]
R(t)	Recovered children	10	10	[27]
$\rho$	Multiplicative factors of breastfeeding children	0.00188	0	[34]
$\psi$	Multiplicative factor of the susceptible children	13.6986	13.6986	[34]
$\alpha$	Multiplicative factor of the vaccinated children	0.002669	0	[34]
$(1 - \rho - \alpha)\psi$	Recruitment rate into susceptible group	13.6363	13.6986	Estimated
$\rho\psi$	Recruitment rate into breastfeeding group	0.02575	0	Estimated
$\alpha\psi$	Recruitment rate into vaccination group	0.03656	0	Estimated
$\Lambda$	Rate of breastfeeding susceptible children	0.22756	0	[35]
$\tau$	Waning rate of maternal antibody from breast milk	0.054945	0.054945	[36]
$\xi$	Vaccination rate of breastfeeding children	0.002	0	Assumed
$\omega$	Vaccination rate of susceptible children	0.038191	0	[36]
$\gamma$	Waning rate of vaccine	0.002778	0	[37]
$\beta SI$	RI transmission rate between infected and susceptible	1.44	1.44	Estimated
$\beta$	RI contact rate	0.0000072	0.0000072	Assumed
$\varepsilon$	Anticipated decline in the RI because of breastfeeding	0.62	0.62	[38]
$\eta$	Expected decrease in the risk of RI because of vaccination	0.71	0.71	[34]
$\mu$	Natural death rate	0.036529	0.036529	[34]
$\phi$	Death rate due to infection	0.004466	0.004466	[39]
$\theta$	Recovery rate due to treatment	0.8333	0.8333	[40]
$\sigma_1$	Constant of incidence transmission saturability for S and I	0.5	0.005	Assumed
$\sigma_2$	Constant of incidence transmission saturability for B and I	0.5	0.005	Assumed
$\sigma_3$	Constant of incidence transmission saturability for V and I	0.4	0.004	Assumed

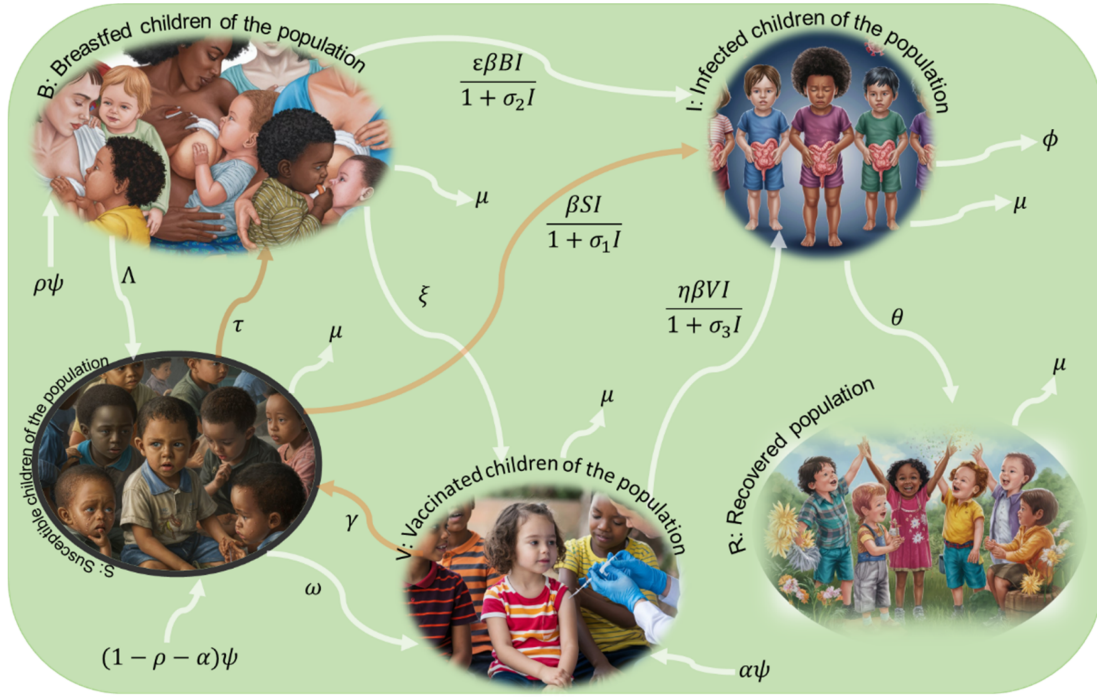


**FIGURE 1** | Flow diagram of rotavirus infection transmission dynamics.

- The vaccinated breastfed population decreases at a rate of  $\xi B$
- Natural deaths reduce the breastfed population at a rate of  $\mu$

To effectively protect the population from rotavirus, children need to be breastfed at a rate that compensates for these losses and helps maintain immunity. The required breastfeeding rate is given by the sum of these factors. By adjusting the breastfeeding rate to meet this requirement, we can help control the spread of rotavirus and protect the population.

To protect the population, children need to be breastfed at the rate of

$$\frac{dB(t)}{dt} = \rho\psi + \Lambda S - \left( \frac{\epsilon\beta I}{1 + \sigma_2 I} + \xi + \tau + \mu \right) B \quad (2b)$$

where  $\xi$  denotes breastfed vaccinated children. The overall rate of vaccination is expressed as:

$$\frac{dV(t)}{dt} = \alpha\psi + \xi B + \omega S - \left( \frac{\eta\beta I}{1 + \sigma_3 I} + \mu + \gamma \right) V \quad (2c)$$

where  $\frac{\eta\beta I}{1 + \sigma_3 I}$  represents infection rate,  $\mu$ , and  $\gamma$  are natural death rate and waning rate of vaccine respectively. The infected population is increased by the susceptible children infected at a rate  $\frac{\beta SI}{1 + \sigma_1 I}$ , breastfed children infected at a rate  $\frac{\epsilon\beta BI}{1 + \sigma_2 I}$ , and vaccinated children infected at a rate  $\frac{\eta\beta VI}{1 + \sigma_3 I}$ . On the other hand, this population reduced by natural death,  $\mu$ , disease-induced death  $\phi$  and recovered due to treatment at a rate  $\theta$ . It follows that the rate of infection of the group is given by:

$$\frac{dI(t)}{dt} = \left( \frac{\beta S}{1 + \sigma_1 I} + \frac{\epsilon\beta B}{1 + \sigma_2 I} + \frac{\eta\beta V}{1 + \sigma_3 I} - (\phi + \theta + \mu) \right) I \quad (2d)$$

The recovered population is increased by the recovered due to treatment at a rate  $\theta$  and decreased due to natural death at a rate  $\mu$ , so that

$$\frac{dR(t)}{dt} = \theta I - \mu R \quad (2e)$$

If the initial conditions of system (2a–2e) are positive, then  $S(0) = S_0 \geq 0$ ;  $B(0) = B_0 \geq 0$ ;  $V(0) = V_0 \geq 0$ ;  $I(0) = I_0 \geq 0$ ;  $R(0) = R_0 \geq 0$ . Since (2a–2e) monitors the human population, the parameters, and all state variables will be positive. Therefore, applying system (1) in (2a–2e), we have

$$N(t) = S(t) + B(t) + V(t) + I(t) + R(t)$$

$$\begin{aligned} N(t) &= (1 - \rho - \alpha)\psi + \tau B + \gamma V - \left( \frac{\beta I}{1 + \sigma_1 I} + \Lambda + \omega + \mu \right) S \\ &+ \rho\psi + \Lambda S - \left( \frac{\epsilon\beta I}{1 + \sigma_2 I} + \xi + \tau + \mu \right) B \\ &+ \alpha\psi + \xi B + \omega S - \left( \frac{\eta\beta I}{1 + \sigma_3 I} + \mu + \gamma \right) V \\ &+ \left( \frac{\beta S}{1 + \sigma_1 I} + \frac{\epsilon\beta B}{1 + \sigma_2 I} + \frac{\eta\beta V}{1 + \sigma_3 I} - (\phi + \theta + \mu) \right) I \\ &+ \theta I - \mu R \end{aligned}$$

$$N(t) = \psi - \mu(S + B + V + I + R) - \phi I.$$

This then resolves into  $(t) \leq \psi - \mu N - \phi I$ .

$$N(t) \leq \psi - \mu N - \phi I \quad (3)$$

At disease-free equilibrium (DFE),  $\phi I = 0$ , so that (3) reduces to

$$N(t) \leq \psi - \mu N \quad (4)$$

Let the integrating factor  $IF = e^{\int \mu dt} = e^{\mu t}$ , then we have from system (4) that

$$N(t) \leq \frac{1}{e^{\mu t}} \left[ \frac{\psi}{\mu} e^{\mu t} + c \right]$$

$$N(t) \leq \frac{\psi}{\mu} + c e^{-\mu t}$$

where  $c$  is the constant of integration. When  $t = 0$ ,  $N(0) = N_1$ , we obtain (5)

$$N_1 - \frac{\psi}{\mu} \leq c$$

Therefore,

$$N(t) \leq \frac{\psi}{\mu} + \left( N_1 - \frac{\psi}{\mu} \right) e^{-\mu t} \quad (5)$$

Applying Birkhoff and Rota's [30] theorem on differential inequality, we get

$$0 \leq N \leq \frac{\psi}{\mu} \text{ as } t \rightarrow \infty$$

This  $N$  would approach the stability point (carrying Capacity) at  $\frac{\psi}{\mu}$ . Therefore, the biologically feasible region

$$\Gamma = \left\{ (S, B, V, I, R) \in \mathbb{R}_+^5 : (S(t) + B(t) + V(t) + I(t) + R(t)) \leq \frac{\psi}{\mu} \right\}$$

is a positively invariant set and attracts all solutions in  $\mathbb{R}_+^5$ . It is sufficient to consider the dynamic system (2a–2e) in the region  $\Gamma$ . It follows that in this region, the model can be considered as being epidemiologically and mathematically well-posed.

## 4.2 | Existence of Equilibrium Points

We proved that the disease-free and endemic equilibrium points are real with respect to the basic reproduction number. Thus, if the basic reproduction number is less than one, then the disease-free equilibrium exists. Also, if the basic reproduction number is greater than one, then the endemic equilibrium exists. Recall that the DFE denotes the point at which the population is free from the virus infection, and the endemic equilibrium is the point at which the virus is resistant in the population. The basic reproduction number of the virus will be considered in the context of the two equilibria.

### 4.2.1 | Disease-Free Equilibrium Point of the System

Observe that the  $R(t)$  exists in isolation from other models in (2a–2e). At DFE, the population is free of infection, then  $I_0 = 0$  and  $R_0 = 0$ . Thus, If we let  $\mathcal{A}_1 = \frac{\beta}{1+\sigma_1 I}$ ,  $\mathcal{A}_2 = \frac{\beta}{1+\sigma_2 I}$ , and  $\mathcal{A}_3 = \frac{\beta}{1+\sigma_3 I}$ . The dynamic attributes are realized using system (6)

$$\left. \begin{aligned} \frac{dS(t)}{dt} &= (1 - \rho - \alpha)\psi + \tau B + \gamma V - (\mathcal{A}_1 I + \Lambda + \omega + \mu)S \\ \frac{dB(t)}{dt} &= \rho\psi + \Lambda S - (\mathcal{A}_2 I + \xi + \tau + \mu)B \\ \frac{dV(t)}{dt} &= \alpha\psi + \xi B + \omega S - (\mathcal{A}_3 I + \mu + \gamma)V \end{aligned} \right\} \quad (6)$$

At the equilibrium state, the rate of change of each variable in (6) becomes zero. Remember  $R(t)$  is the recovered children and since there is no infection, then  $R(t)$  will be eliminated thus, resulting in (7)

$$\frac{dS(t)}{dt} = \frac{dB(t)}{dt} = \frac{dV(t)}{dt} = 0 \quad (7)$$

The corresponding closed-form equilibrium parameters can be expressed as

$$E_0 = (S_0, B_0, V_0, I_0, R_0) = \left( \frac{\psi [\beta_1 r_1 - \rho \mu r_4]}{\mu [r_3 r_2 + \tau r_1 + \gamma \Lambda]}, \frac{\psi [\rho \mu r_1 + \Lambda \beta_1]}{\mu [r_3 r_2 + \tau r_1 + \gamma \Lambda]}, \frac{\psi [\alpha \mu r_2 + \xi \beta_2 + \omega \beta_3]}{\mu [r_3 r_2 + \tau r_1 + \gamma \Lambda]}, 0, 0 \right) \quad (8)$$

where  $r_1 = \xi + \tau + \mu$ ,  $r_2 = \xi + \tau + \mu + \Lambda$ ,  $r_3 = \xi + \mu$ ,  $r_4 = \xi + \gamma + \mu$ ,  $\beta_1 = \mu + \gamma - \alpha\mu$ ,  $\beta_2 = \rho\mu + \Lambda + \omega$ ,  $\beta_3 = \tau + \mu - \rho\mu$ ,  $r_1' = \omega + \gamma + \mu$ , and  $r_2' = \Lambda + \omega + \gamma + \mu$ . Notice that we have introduced  $r_1, r_2, r_3, r_4, \beta_1, \beta_2, \beta_3, r_1',$  and  $r_2'$  in (8) for notational convenience and will be used throughout the remaining parts of the paper.

### 4.2.2 | Basic Reproduction Number (BRN)

The BRN of the virus is the anticipated number of subsequent cases brought on by a single infection in a population that is entirely susceptible [41]. The BRN is important to analyze endemic disease in Biomedical models. Let  $R_{BV}$  denote the basic reproduction number of model system (2a–2e) in the presence of  $B$  and  $V$ . When  $B$  and  $V$  are not included, the model gives the BRN as  $R_0$ , that is, the transmission rate of rotavirus infection by a single infected child in the absence of breastfeeding and vaccination. Using the next-generation matrix [41], we derive the BRN in the presence of  $B$  and  $V$  as

$$F = \begin{bmatrix} 0 & 0 & 0 \\ 0 & 0 & 0 \\ \beta\psi[(r_1)(\beta_1) - \rho\mu(r_4)] \\ + \varepsilon\beta\psi[\rho\mu(r_1) + \Lambda(\beta_1)] \\ 0 & 0 & \frac{+\eta\beta\psi[\alpha\mu(r_2) + \xi(\beta_2) + \omega(\beta_3)]}{\mu[(r_3)(r_2) + \tau(r_1) + \gamma\Lambda]} \end{bmatrix}, \quad V_1 = \begin{bmatrix} r_4 & 0 & \varepsilon\beta B_0 \\ -\xi & \mu + \gamma & \eta\beta V_0 \\ 0 & 0 & \phi + \theta + \mu \end{bmatrix}$$

The matrix  $F$  corresponds to the transmission part and it describes the number of ways that new rotavirus infection can arise. The matrix  $V_1$  corresponds to transition part, which describes the number of ways that individuals can move between compartments, and it includes removal by death.

It follows that

$$FV_1^{-1} = \begin{bmatrix} 0 & 0 & 0 \\ 0 & 0 & 0 \\ \beta\psi[(\xi + \tau + \mu)(\mu + \gamma - \alpha\mu) - \rho\mu(\xi + \gamma + \mu)] \\ + \varepsilon\beta\psi[\rho\mu(\omega + \gamma + \mu) + \Lambda(\mu + \gamma - \alpha\mu)] \\ 0 & 0 & \frac{+\eta\beta\psi[\alpha\mu(\xi + \tau + \mu + \Lambda) + \xi(\rho\mu + \Lambda + \omega) + \omega(\tau + \mu - \rho\mu)]}{\mu[(\xi + \mu)(\Lambda + \omega + \gamma + \mu) + \tau(\omega + \gamma + \mu) + \gamma\Lambda][\mu + \theta + \phi]} \end{bmatrix}$$

$FV_1^{-1}$  is the product of transmission  $F$  and inverse of transition  $V_1^{-1}$  which is used in computing the basic reproduction number (9).

$$R_{BV} = \frac{\beta\psi}{\mu(\phi + \theta + \mu)} \left[ \frac{[(\xi + \tau + \mu)(\mu + \gamma - \alpha\mu) - \rho\mu(\xi + \gamma + \mu)] + \varepsilon[\rho\mu(\omega + \gamma + \mu) + \Lambda(\mu + \gamma - \alpha\mu)] + \eta[\alpha\mu(\xi + \tau + \mu + \Lambda) + \xi(\rho\mu + \Lambda + \omega) + \omega(\tau + \mu - \rho\mu)]}{[(\xi + \mu)(\Lambda + \omega + \gamma + \mu) + \tau(\omega + \gamma + \mu) + \gamma\Lambda]} \right] \quad (9)$$

The BRN in the absence of  $B$  and  $V$  can be obtained by setting the parameters relating to  $B$  and  $V$  to zero, (i.e.,  $\Lambda = \tau = \rho = \xi = \omega = \gamma = \alpha = 0$ ); we then have (10)

$$R_0 = \frac{\beta\psi}{\mu(\phi + \theta + \mu)} \quad (10)$$

To obtain the reproduction number in the absence of either  $B$  or  $V$ , we set the parameters relating to either  $B$  or  $V$  to zero. Then, we obtain the BRN in the presence of  $V$  or  $B$  respectively. For the BRN in the presence of  $V$  only, we set the parameters relating to  $B$  to zero, that is,  $\rho = \Lambda = \tau = \xi = 0$ , and obtain (11)

$$R_V = \frac{\beta\psi}{\mu(\phi + \theta + \mu)} \left[ \frac{\omega(\mu + \alpha\mu^2) + \mu(\gamma + \mu + \alpha\mu)}{\mu(\omega + \gamma + \mu)} \right] \quad (11)$$

While in the presence of  $B$  only, we set the parameters relating to  $V$  to zero, that is,  $\alpha = \omega = \gamma = \xi = 0$  and we get

$$R_B = \frac{\beta\psi}{\mu(\phi + \theta + \mu)} \left[ \frac{(\mu + \tau)\mu - \rho\mu^2 + \varepsilon\mu(\rho\mu + \Lambda)}{[\tau\mu + \mu(\mu + \Lambda)]} \right] \quad (12)$$

Using (10) we can express (9), (11), and (12) as

$$R_{BV} = R_0 \left[ \frac{[(\xi + \tau + \mu)(\mu + \gamma - \alpha\mu) - \rho\mu(\xi + \gamma + \mu)] + \varepsilon[\rho\mu(\omega + \gamma + \mu) + \Lambda(\mu + \gamma - \alpha\mu)] + \eta[\alpha\mu(\xi + \tau + \mu + \Lambda) + \xi(\rho\mu + \Lambda + \omega) + \omega(\tau + \mu - \rho\mu)]}{[(\xi + \mu)(\Lambda + \omega + \gamma + \mu) + \tau(\omega + \gamma + \mu) + \gamma\Lambda]} \right] \quad (13)$$

$$R_V = R_0 \left[ \frac{\omega(\mu + \alpha\mu^2) + \mu(\gamma + \mu + \alpha\mu)}{\mu(\omega + \gamma + \mu)} \right] \quad (14)$$

$$R_B = R_0 \left[ \frac{(\mu + \tau)\mu - \rho\mu^2 + \varepsilon\mu(\rho\mu + \Lambda)}{[\tau\mu + \mu(\mu + \Lambda)]} \right] \quad (15)$$

Equations (13), (14), and (15) represent the relationship between  $R_{BV}$  and  $R_0$ ,  $R_V$ , and  $R_0$ , and  $R_B$  and  $R_0$ , respectively and the efficiency of controls used in this paper. Therefore  $R_{BV}$  is the required basic reproduction number for our model and hence we conclude that both  $B$  and  $V$  will be effective in controlling RI. This is because  $R_{BV}$  is the best-case scenario, that is  $R_{BV} < R_V < R_B < R_0$ . Thus, if  $R_{BV} < 1$ , then RI will not spread within the population. But if  $R_{BV} > 1$ , the infection then spreads among the populace.

**TABLE 2** | Number of possible positive roots of  $F(I^*)$  for  $R_{BV} > 1$ .

Cases	$a_1$	$a_2$	$a_3$	$a_4$	$R_{BV}$	No of sign change	No of positive roots
1	+	+	+	-	$R_{BV} > 1$	1	1
2	+	-	-	-	$R_{BV} > 1$	1	1
3	+	-	+	-	$R_{BV} > 1$	3	1, 3
4	1	-	-	-	$R_{BV} > 1$	1	1

#### 4.2.3 | Endemic Equilibrium Point (EEP)

The EEP,  $E^*$ , is the point where rotavirus infection cannot be eradicated but remains in the population. For the disease to persist in the population,  $E^* \neq 0$ , that is:

$$E^* = (S^*, B^*, V^*, I^*, R^*) \neq 0$$

We shall establish the existence of the endemic equilibrium point of this study using Lemma 1 below.

**Lemma 1.** *There exists a positive equilibrium point if  $R_{BV} > 1$ .*

*Proof.* See Appendix A, that is, from Equations (A1–A6).  $\square$

Observe that (A6) can be rewritten as

$$a_1 I^{*3} + a_2 I^{*2} + a_3 I^* + a_4 = 0 \quad (16)$$

where  $a_4$  can also be rewritten as  $R_{BV} - 1$ . From (16),  $a_1$  is positive as shown in (A6) and we cannot state whether  $a_2$ ,  $a_3$ , and  $a_4$  are either positive or negative. It follows that  $a_4 > 0$  whenever  $R_{BV} > 1$ , thus the number of positive real roots for (16) depends on the signs of  $a_2$  and  $a_3$ . The Equation (16) can be analyzed using the Discartes rule of signs on polynomial functions such as in (17). For example, let.

$$F(I^*) = a_1 I^{*3} + a_2 I^{*2} + a_3 I^* + a_4 \quad (17)$$

the different possibilities for the roots of  $F(I^*)$  are tabulated in Table 2.

Equations (2a–2e) has a unique EEP where Table 2 satisfies cases 1, 2, and 4 respectively. The existence of multiple, that is, more than one EEP when  $R_{BV} > 1$  and Case 3 are satisfied. Therefore, (2) will always exhibit an EEP whenever  $R_{BV} > 1$ .

### 4.3 | Stability Analysis of Equilibria

#### 4.3.1 | Local Stability of Disease-Free Equilibrium

**Theorem 1.** *The disease-free equilibrium (DEF) is locally asymptotically stable if  $R_{BV} < 1$  and unstable if  $R_{BV} > 1$ .*

*Proof.* To prove the stability of the proposed SBVIR model from the DFE of  $E_0 = (S_0, B_0, V_0, I_0, R_0)$ , we linearize system (2a–2e) of the dynamic system by determining the Jacobian matrix  $J(E_0)$  thus



$$J(E_0) = \begin{bmatrix} -(\Lambda + \omega + \mu) & \tau & \gamma & \beta S_0 \\ \Lambda & -(\xi + \tau + \mu) & 0 & -\varepsilon \beta B_0 \\ \omega & \xi & -(\mu + \gamma) & -\eta \beta V_0 \\ 0 & 0 & 0 & (R_{BV} - 1)(\phi + \theta + \mu) \end{bmatrix}$$

The characteristic equation of  $J(E_0)$  of (2a–2e) at  $E_0$  is of the form  $|J(E_0) - \lambda I| = 0$  which results into

$$\lambda^4 + d_1 \lambda^3 + d_2 \lambda^2 + d_3 \lambda + d_4 = 0 \quad (18)$$

□

where

$$d_1 = (1 - R_{BV})(\phi + \theta + \mu) + (\Lambda + \omega + \mu) + (\xi + \tau + \mu) + (\mu + \gamma)$$

$$d_2 = (1 - R_{BV})(\phi + \theta + \mu)((\Lambda + \omega + \mu) + (\xi + \tau + \mu) + (\mu + \gamma)) + \Lambda(\xi + \mu) + (\omega + \mu)(\xi + \tau + \mu) + \mu(\Lambda + \omega + \mu) + \gamma(\Lambda + \mu) + (\xi + \tau + \mu)(\mu + \gamma)$$

$$d_3 = (1 - R_{BV})(\phi + \theta + \mu)(\Lambda(\xi + \mu) + (\omega + \mu)(\xi + \tau + \mu) + \mu(\Lambda + \omega + \mu) + \gamma(\Lambda + \mu) + (\xi + \tau + \mu)(\mu + \gamma)) + \mu\Lambda\xi + \mu(\mu + \gamma) + \mu(\omega + \mu)(\xi + \tau + \mu) + \gamma\mu(\xi + \tau + \mu)$$

$$d_4 = (1 - R_{BV})(\phi + \theta + \mu)(\mu\Lambda\xi + \mu(\mu + \gamma) + \mu(\omega + \mu)(\xi + \tau + \mu) + \gamma\mu(\xi + \tau + \mu)).$$

We observe in (18) that  $d_1 > 0$ ,  $d_3 > 0$  and  $d_4 > 0$  are automatically satisfied if  $R_{BV} < 0$ . Also,  $d_1 d_2 d_3 - (d_3^2 + d_2^2 d_4) > 0$ . Hence, by Routh-Hurwitz criterion we have that all roots of (24) have negative real parts. Thus, the disease-free equilibrium point  $E_0$  is locally asymptotically stable for  $R_{BV} < 0$  which agrees with findings in [30, 42].

#### 4.3.2 | Local Stability of the Endemic Equilibrium Point

Next, we compute the local stability of the endemic equilibrium  $E^*$  of the system (2a–2e)

**Theorem 2.** *The endemic equilibrium points  $E^*$  of the system (2a–2e) is locally asymptotically stable if  $R_{BV} > 1$ .*

*Proof.* Suppose that  $R_{BV} > 1$ , we linearize system (2a–2e) by determining the Jacobian matrix at the endemic equilibrium point  $E^*(S^*, B^*, V^*, I^*, R^*)$ .

$$J(E^*) = \begin{bmatrix} -(\nu_2 - \gamma) & \tau & \gamma & -\mathcal{A}_1^{2\ddagger} S^* \\ \Lambda & -r_2 & 0 & -\varepsilon \mathcal{A}_2^{2\ddagger} B^* \\ \omega & \xi & -(r_4 - \xi) & -\eta \mathcal{A}_3^{2\ddagger} B^* \\ -\mathcal{A}_1^{2\ddagger} I^* & -\varepsilon \mathcal{A}_2^{2\ddagger} I^* & -\eta \mathcal{A}_3^{2\ddagger} I^* & (R_{BV} - 1)(\phi + \theta + \mu) \end{bmatrix} \quad (19)$$

where  $\mathcal{A}_1^{2\ddagger} = \beta/(1 + \sigma_1 I^*)^2$ ,  $\mathcal{A}_2^{2\ddagger} = \beta/(1 + \sigma_2 I^*)^2$  and  $\mathcal{A}_3^{2\ddagger} = \beta/(1 + \sigma_3 I^*)^2$ . From (19), the characteristic equation of the Jacobian matrix of system (2) at  $E^*$  is of the form  $|J(E^*) - \lambda I| = 0$  and can be simplified to Equation (20) (See Appendix B).

$$\lambda^4 + k_1 \lambda^3 + k_2 \lambda^2 + k_3 \lambda + k_4 = 0 \quad (20)$$

□

We observe that  $k_1 > 0$ ,  $k_2 > 0$ ,  $k_3 > 0$  and  $k_4 > 0$  will be positive if  $R_{BV} > 1$  and  $k_1 k_2 k_3 - (k_3^2 + k_1^2 k_4) > 0$  is also, satisfied if  $R_{BV} > 1$ . From the Routh-Hurwitz theorem, we know that all roots of (20) have negative real parts. Thus, the endemic equilibrium point  $E^*$  is locally asymptotically stable for  $R_{BV} > 1$  [35, 43].

#### 4.3.3 | Global Stability of Equilibria

The global stability of equilibria determines the point at the rotavirus interior. Considering the DFE,  $E_0$ , the global stability is validated with the Lyapunov function [42, 44].

**Theorem 3.** *The DFE of the system (2a–2e) is universally stable asymptotically in  $\Gamma$  if  $R_{BV} < 1$ , where  $\Gamma$ , is the feasible region of system (2a–2e).*

*Proof.* We construct the following Lyapunov function as

$$\mathcal{L} : \{(S, B, V, I, R) \in \Gamma\} \rightarrow \mathbb{R} \text{ by } \mathcal{L}(S, B, V, I, R) = (\xi + \tau + \mu)(\mu + \gamma)I \quad (21)$$

□

Then, differentiating (21) with time  $t$ , we have

$$\begin{aligned} \dot{\mathcal{L}} &= (\xi + \tau + \mu)(\mu + \gamma)[\mathcal{A}_1 SI + \mathcal{A}_2 \varepsilon BI + \eta \mathcal{A}_3 VI - (\phi + \theta + \mu)I] \\ &= (\xi + \tau + \mu)(\mu + \gamma) \left[ \beta \left( \frac{S}{1 + \sigma_1 I} + \frac{\varepsilon B}{1 + \sigma_2 I} + \frac{\eta V}{1 + \sigma_3 I} \right) I - (\phi + \theta + \mu)I \right] \\ &\leq (\xi + \tau + \mu)(\mu + \gamma)[\beta(S + \varepsilon B + \eta V) - (\phi + \theta + \mu)]I \\ &< (\xi + \tau + \mu)(\mu + \gamma)[\beta(S + B + V + I + R) - (\phi + \theta + \mu)]I \\ &= (\xi + \tau + \mu)(\mu + \gamma) \left[ \beta \frac{\Psi}{\mu} - (\phi + \theta + \mu) \right] I \\ &= (R_0 - 1)(\xi + \tau + \mu)(\mu + \gamma)I \end{aligned}$$

Since  $R_{BV} < R_0$ , in  $\varepsilon, \eta \in (0, 1)$ , these yields

$$\dot{\mathcal{L}} < (R_{BV} - 1)(\xi + \tau + \mu)(\mu + \gamma)I$$

Therefore, if  $R_{BV} < 1$ , then the DFE is universally stable asymptotically in the feasible region  $\Gamma$ .

## 5 | Results

Numerical simulation is employed to verify the theoretical predictions discussed in Section 4. The Runge-Kutta method of order four (RK4) is applied using MATLAB computational engine [45]. Dynamic behavior of rotavirus infection is studied using a distinct set of parameter values. Also, some of the parameter values and the initial data were obtained from [26, 43], [31, 45–49]. The BRN in the presence of  $B$  and  $V$  were simulated using the parameters  $\rho$  and  $\alpha$ , and the results were demonstrated in Figures 2, 3, and 4 respectively. It was observed that both  $B$  and  $V$  reduces the value of  $R_{BV}$  effectively. In this case, vaccination provides a stronger preventive measure than breastfeeding.

Notice that integrated control works more efficiently than either of the controls. When  $\beta = 0.0072$ , the value of  $R_0 = 2.9525 >$

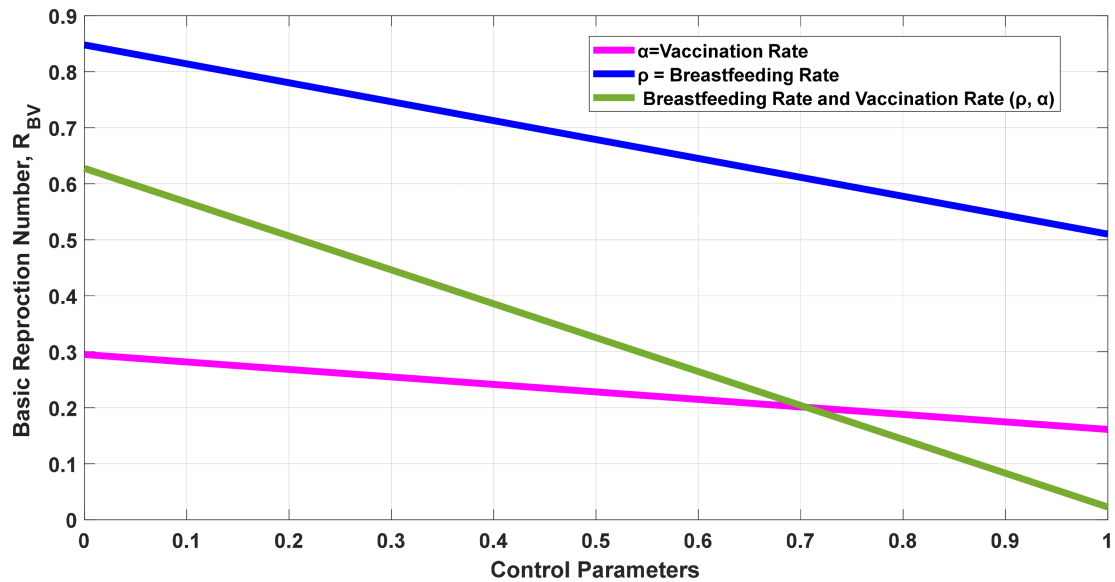


**FIGURE 2** | Numerical simulation of the basic reproduction number in the presence of  $B$  and  $V$  with parameter values  $\psi = 13.6986$ ,  $\tau = 0.054945$ ,  $\gamma = 0.002778$ ,  $\xi = 0.002$ ,  $\theta = 0.8333$ ,  $\phi = 0.04466$ ,  $\Lambda = 0.22756$ ,  $\omega = 0.038191$ ,  $\beta = 0.0072$ ,  $\varepsilon = 0.00062$ ,  $\eta = 0.00071$ ,  $\mu = 0.036529$ , while  $\alpha$  and  $\rho$  respectively ranges from 0 to 1.

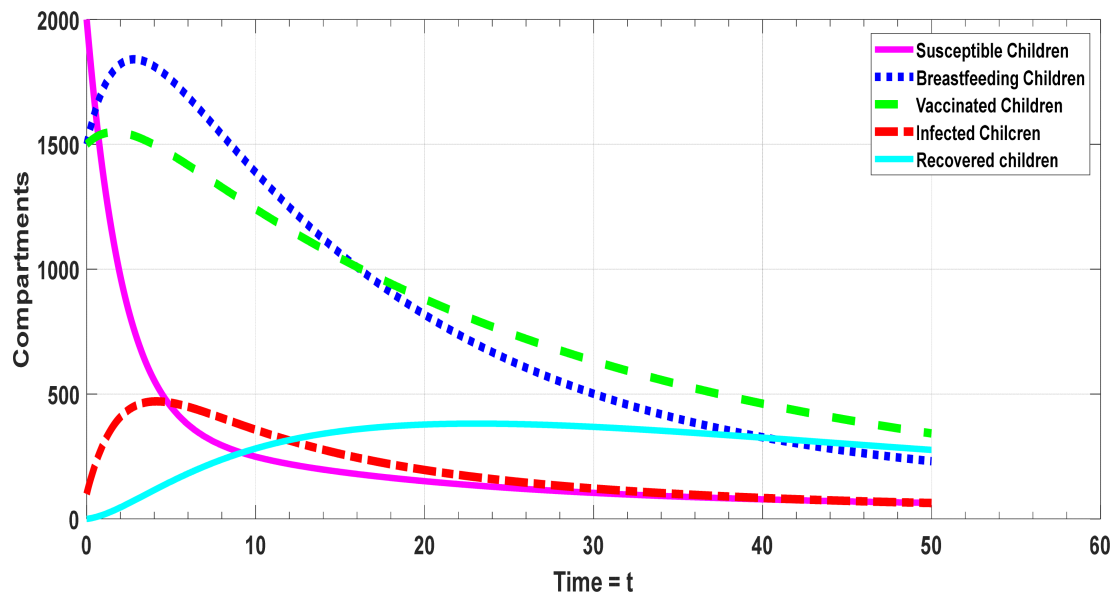


**FIGURE 3** | Numerical simulation of model Equations (2a–2e) on the effect of breastfeeding newborn children ( $\rho = 0.0018$ ) in the control of RI where  $\psi = 13.6986$ ,  $\rho = 0.0018$ ,  $\alpha = 0.002669$ ,  $\tau = 0.054945$ ,  $\gamma = 0.002778$ ,  $\xi = 0.002$ ,  $\theta = 0.8333$ ,  $\phi = 0.04466$ ,  $\Lambda = 0.22756$ ,  $\omega = 0.038191$ ,  $\mu = 0.036529$ ,  $\beta = 0.072$ ,  $\sigma_1 = 0.5$ ,  $\varepsilon = 0.00062$ ,  $\sigma_2 = 0.5$ ,  $\eta = 0.00071$ ,  $\sigma_3 = 0.4$  and the initial variables  $S_0 = 2000$ ,  $B_0 = 1500$ ,  $V_0 = 1500$ ,  $I_0 = 100$  and  $R_0 = 10$ .

1 and  $R_{BV} = 0.65115 < 1$ . From this fact, we observe that the value of

$$\frac{[(\xi + \tau + \mu)(\mu + \gamma - \alpha\mu) - \rho\mu(\xi + \gamma + \mu)] + \varepsilon[\rho\mu(\omega + \gamma + \mu) + \Lambda(\mu + \gamma - \alpha\mu)] + \eta[\alpha\mu(\xi + \tau + \mu + \Lambda) + \xi(\rho\mu + \Lambda + \omega) + \omega(\tau + \mu - \rho\mu)]}{[(\xi + \mu)(\Lambda + \omega + \gamma + \mu) + \tau(\omega + \gamma + \mu) + \gamma\Lambda]} = 0.22054 < 1$$

therefore,  $R_{BV} < R_0$ . This simply shows that the combined effect of  $B$  and  $V$  can reduce the spread of RI in the population. The disease-free equilibrium point is locally and globally stable at

$E_0 = (82.51, 202.23, 91.34, 0, 0)$ . The eventual eradication of the disease from the population is seen from an epidemiological perspective.

Figure 2 illustrates the impact of  $V$  and  $B$ , separately, on the Basic Reproduction Number (BRN) of the infection and the combined effect of  $V$  and  $B$  on the BRN. Notably, we observed that the BRN value is less than one when  $V$  or  $B$  is the only control and when  $B$  and  $V$  are combined. The observed reduction in BRN signifies a decrease in the rate at which one infected child transmits rotavirus infection within the population. The combined effect of  $B$  and  $V$  had the most significant positive influence

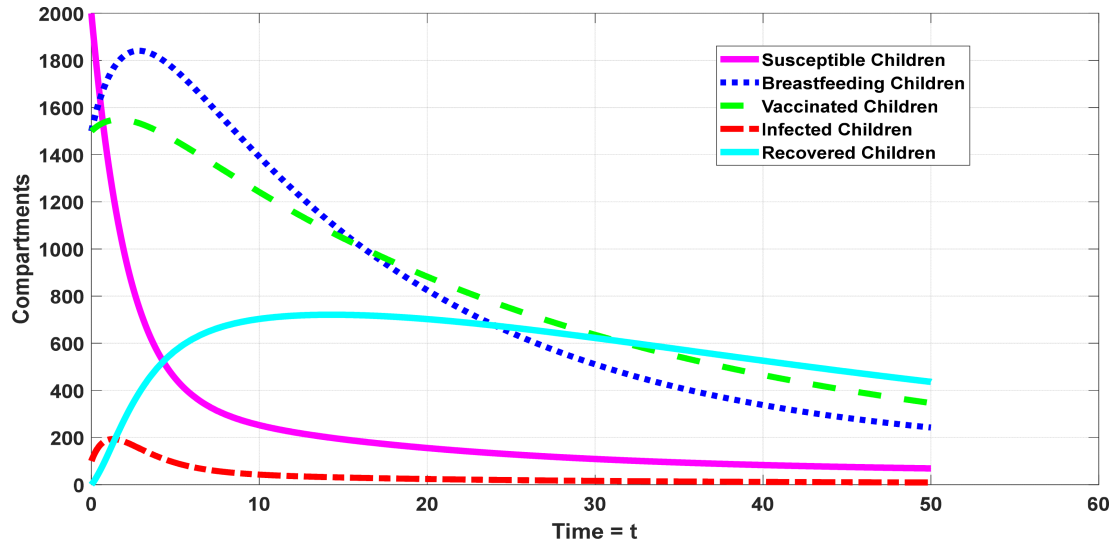


**FIGURE 4** | Numerical simulation of model Equations (2a–2e) on the effect of breastfeeding newborn children ( $\rho = 0.00188$ ) in the control of RI where  $\psi = 13.6986$ ,  $\rho = 0.00188$ ,  $\alpha = 0.002669$ ,  $\tau = 0.054945$ ,  $\gamma = 0.002778$ ,  $\xi = 0.002$ ,  $\theta = 0.8333$ ,  $\phi = 0.04466$ ,  $\Lambda = 0.22756$ ,  $\omega = 0.038191$ ,  $\mu = 0.036529$ ,  $\beta = 0.072$ ,  $\sigma_1 = 0.5$ ,  $\varepsilon = 0.00062$ ,  $\sigma_2 = 0.5$ ,  $\eta = 0.00071$ ,  $\sigma_3 = 0.4$  and the initial variables  $S_0 = 2000$ ,  $B_0 = 1500$ ,  $V_0 = 1500$ ,  $I_0 = 100$  and  $R_0 = 10$ .

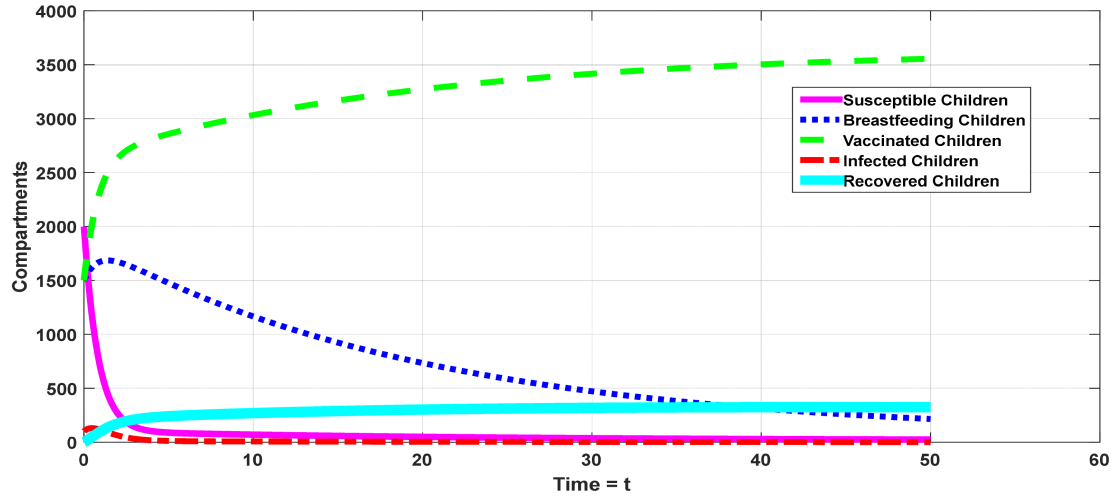


**FIGURE 5** | Numerical simulation of model Equations (2a–2e) on the effect of vaccination on susceptible children ( $\omega$ ) in the control of RI where  $\psi = 13.6986$ ,  $\rho = 0.0018$ ,  $\alpha = 0.002669$ ,  $\tau = 0.054945$ ,  $\gamma = 0.002778$ ,  $\xi = 0.002$ ,  $\theta = 0.8333$ ,  $\phi = 0.4466$ ,  $\Lambda = 0.22756$ ,  $\omega = 0.8191$ ,  $\mu = 0.036529$ ,  $\beta = 0.072$ ,  $\sigma_1 = 0.5$ ,  $\varepsilon = 0.00062$ ,  $\sigma_2 = 0.5$ ,  $\eta = 0.00071$ ,  $\sigma_3 = 0.4$  and the initial variables  $S_0 = 2000$ ,  $B_0 = 1500$ ,  $V_0 = 1500$ ,  $I_0 = 100$  and  $R_0 = 10$ .

on diminishing RI transmission dynamics. Turning our attention to Figures 3 and 4, we can observe a decline in the number of susceptible children, while breastfed, vaccinated, infected, and recovered children exhibited oscillations before stabilizing. Importantly, Figure 4 shows an increased reduction in the number of infected children. This outcome can be attributed to a slight increase in the population of breastfeeding children, suggesting that the prevalence of rotavirus can be minimized in the population through effective breastfeeding practices.

The impact of vaccinating susceptible children and the combination of breastfeeding and vaccination rates on the dynamics of rotavirus infection are depicted in Figures 5 and 6, respectively. It was observed that vaccination of susceptible children in Figure 5 had a significant effect, resulting in a reduction in the number of infections compared to breastfeeding in Figure 4.

Furthermore, the combination of breastfeeding and vaccination positively influenced the dynamics of rotavirus infection; in other words, the more children were breastfed and vaccinated (leading to an increase in  $\rho$  and  $\alpha$ ), the fewer children were infected with rotavirus. Figure 7 illustrates the combined effect of breastfeeding and vaccination on different compartments of the SBVIR model. An increase in the number of breastfeeding and vaccinated children led to a substantial reduction in the number of infected children, consequently increasing the number of children who recovered from RI. This implies that the combination of breastfeeding and vaccination is more effective in controlling RI.

Figure 8 demonstrates the effect of vaccinating and breastfeeding newborns and susceptible children on the dynamics of RI in the population. It was observed that a slight increase in parameters associated with breastfeeding and vaccination

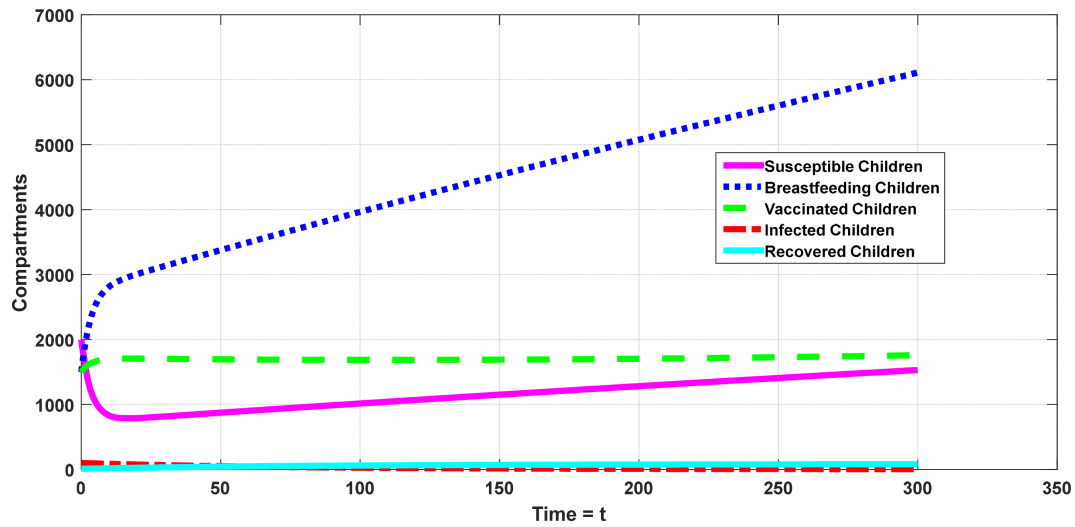


**FIGURE 6** | Numerical simulation of model Equations (2a–2e) on the effect of breastfeeding and vaccination on the newly born children ( $\rho$  and  $\alpha$ ) in the control of RI where  $\psi = 13.6986$ ,  $\rho = 0.00188$ ,  $\alpha = 0.005$ ,  $\tau = 0.054945$ ,  $\gamma = 0.002778$ ,  $\xi = 0.002$ ,  $\theta = 0.0095$ ,  $\phi = 0.004466$ ,  $\Lambda = 0.22756$ ,  $\omega = 0.001884$ ,  $\mu = 0.0002537$ ,  $\beta = 0.0000072$ ,  $\sigma_1 = 0.5$ ,  $\varepsilon = 0.62$ ,  $\sigma_2 = 0.5$ ,  $\eta = 0.71$ ,  $\sigma_3 = 0.4$  and the initial variables  $S_0 = 2000$ ,  $B_0 = 1500$ ,  $V_0 = 1500$ ,  $I_0 = 100$  and  $R_0 = 10$ .

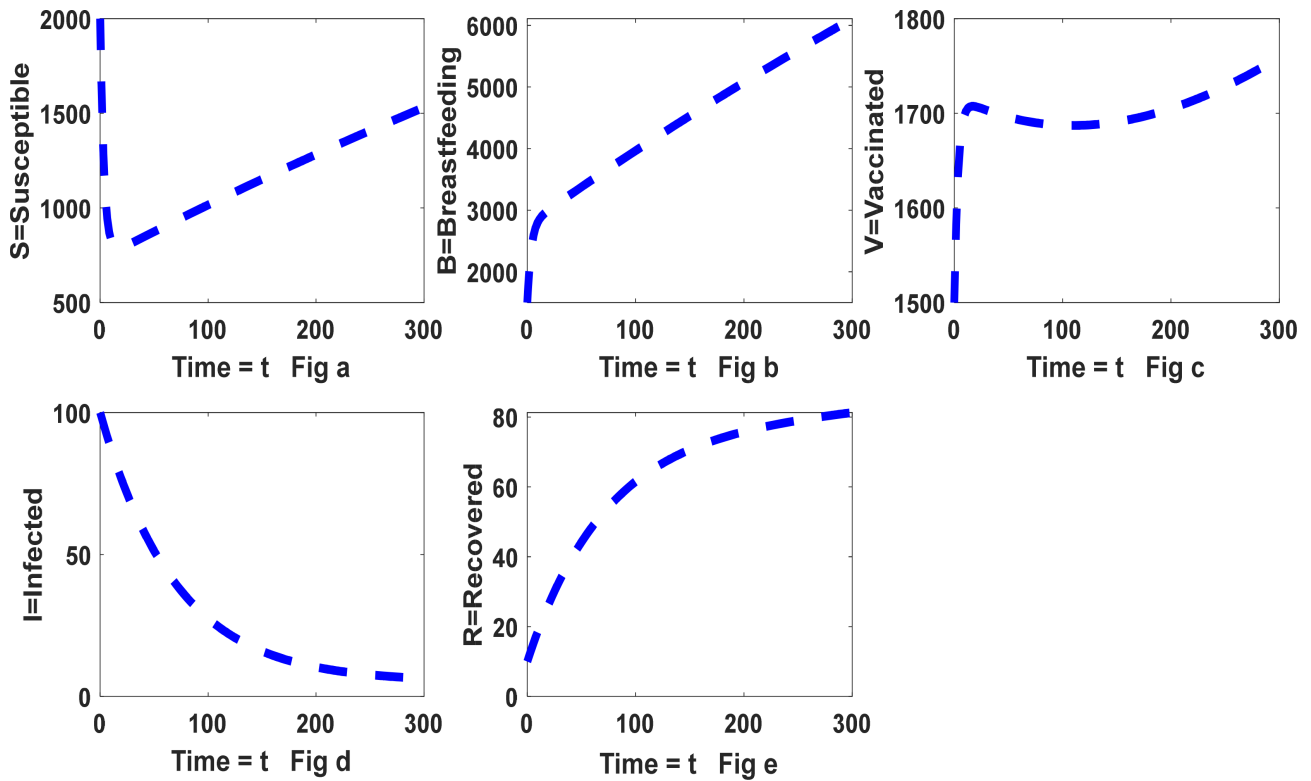


**FIGURE 7** | Numerical simulation Equations (2a–2e) on the effect of breastfeeding on both the newly born and susceptible children ( $\rho$  and  $\alpha$ ) in the control of RI where (i.e., individual groups were displayed) and  $\psi = 13.6986$ ,  $\rho = 0.00188$ ,  $\alpha = 0.005$ ,  $\tau = 0.054945$ ,  $\gamma = 0.002778$ ,  $\xi = 0.002$ ,  $\theta = 0.0095$ ,  $\phi = 0.004466$ ,  $\Lambda = 0.22756$ ,  $\omega = 0.001884$ ,  $\mu = 0.02537$ ,  $\beta = 0.0000072$ ,  $\sigma_1 = 0.5$ ,  $\varepsilon = 0.62$ ,  $\sigma_2 = 0.5$ ,  $\eta = 0.71$ ,  $\sigma_3 = 0.4$  and the initial variables  $S_0 = 2000$ ,  $B_0 = 1500$ ,  $V_0 = 1500$ ,  $I_0 = 100$  and  $R_0 = 10$ .

(i.e.,  $\alpha$ ,  $\rho$ ,  $\omega$ ,  $\Lambda$  and  $\Lambda$ ) could lead to the eradication of RI. Figures 9 and 10 respectively illustrate the effects of vaccination and breastfeeding on the dynamics of the infection. The results indicate that both factors play crucial roles in preventing and eradicating RI in the population, with vaccination having a greater impact on the dynamics of the infection. This could be attributed to the fact that maternal antibodies in humans tend to decrease over a period of 6

to 12 months. In other words, immunity in newborn babies is only temporary and starts to decline after the first few months. Therefore, it is essential to commence childhood vaccinations when the baby is 2 months old.

The effect of saturated constants on the infected group was shown in Figure 11 using different values such as  $\sigma_1 = \sigma_2 = \sigma_3 = 0.5$ ,



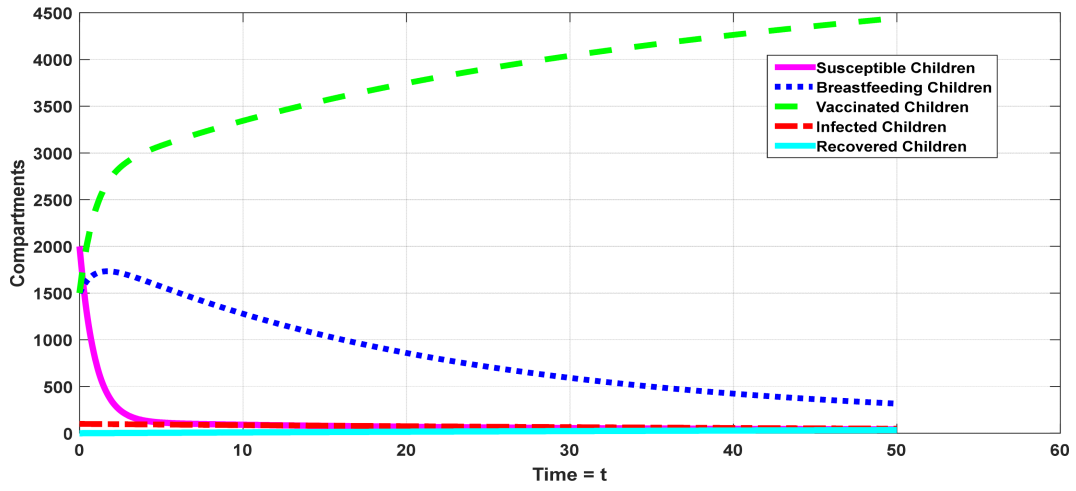


**FIGURE 8** | Numerical simulation of model Equations (2a–2e) on the effect of vaccination and breastfeeding on both the newly born and susceptible children in controlling RI ( $\rho, \omega, \Lambda, \alpha$  and  $\xi$ ) where  $\psi = 13.6986$ ,  $\rho = 0.00188$ ,  $\alpha = 0.005$ ,  $\tau = 0.054945$ ,  $\gamma = 0.002778$ ,  $\xi = 0.0025$ ,  $\theta = 0.0095$ ,  $\phi = 0.004466$ ,  $\Lambda = 0.23756$ ,  $\omega = 0.8191$ ,  $\mu = 0.0002537$ ,  $\beta = 0.0000072$ ,  $\sigma_1 = 0.5$ ,  $\varepsilon = 0.00062$ ,  $\sigma_2 = 0.5$ ,  $\eta = 0.00071$ ,  $\sigma_3 = 0.4$  and the initial variables  $S_0 = 2000$ ,  $B_0 = 1500$ ,  $V_0 = 1500$ ,  $I_0 = 100$  and  $R_0 = 10$ .

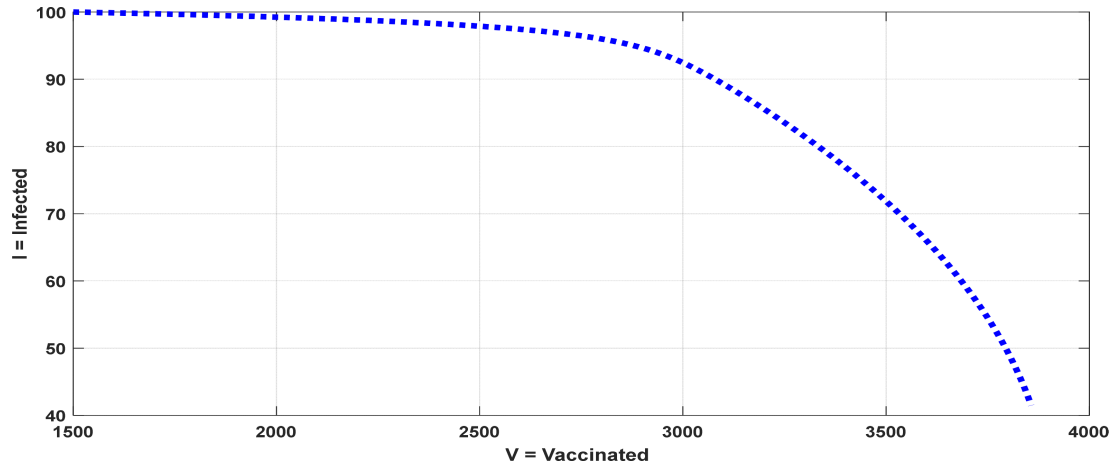


**FIGURE 9** | Dynamic behavior of the system (2a–2e) on the effect of  $V$  on RI.

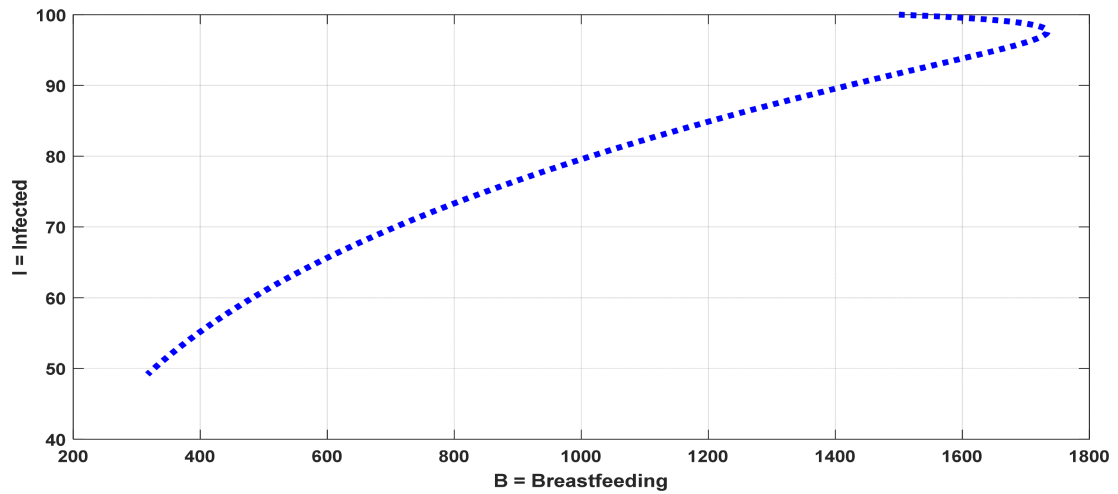


**FIGURE 10** | Dynamic response of the system (2a–2e) on the effect of  $B$  on the infection.

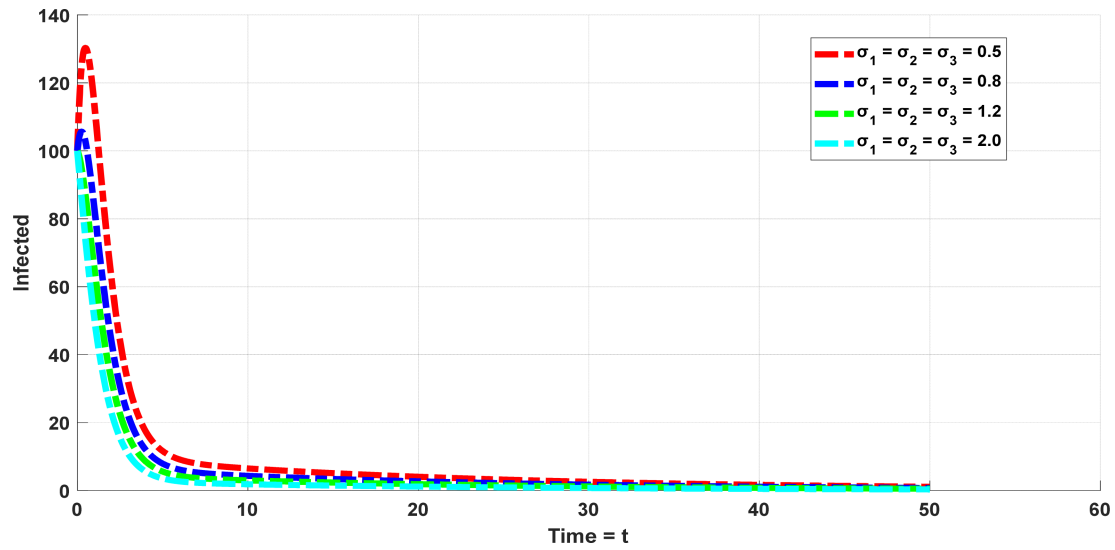


**FIGURE 11** | Effect of the saturated incidence rate on RI dynamics using model system (2a–2e), that is, from  $\sigma_1 = \sigma_2 = \sigma_3 = 0.5$  to  $\sigma_1 = \sigma_2 = \sigma_3 = 2.0$ .

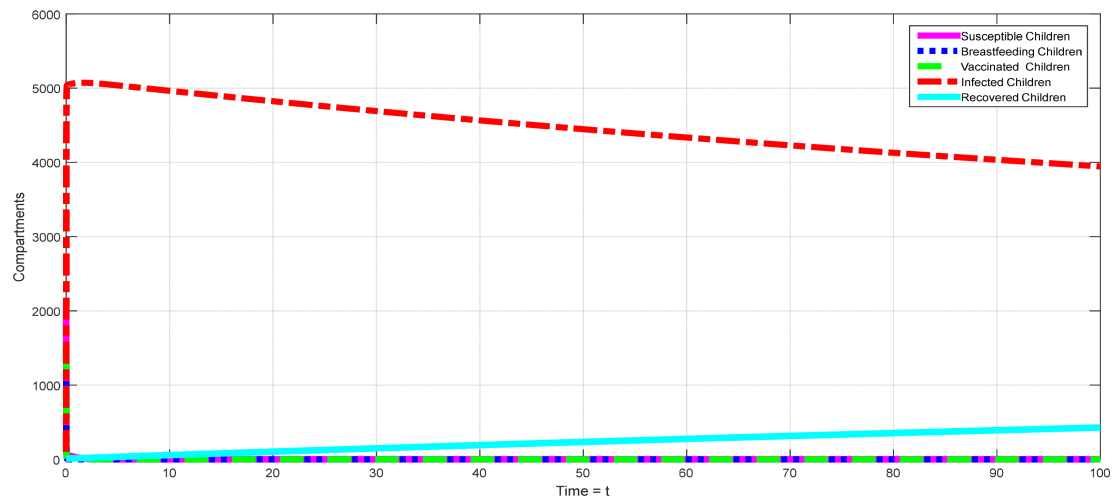


**FIGURE 12** | Numerical simulation of model Equations (2a–2e) when there is no vaccination and breastfeeding of children on RI {where  $\psi = 13.6986$ ,  $\rho = 0$ ,  $\alpha = 0$ ,  $\tau = 0.054945$ ,  $\gamma = 0.002778$ ,  $\xi = 0$ ,  $\theta = 0.00095$ ,  $\phi = 0.004466$ ,  $\Lambda = 0$ ,  $\omega = 0.038191$ ,  $\mu = 0.00002537$ ,  $\beta = 0.72$ ,  $\sigma_1 = 0.005$ ,  $\epsilon = 0.62$ ,  $\sigma_2 = 0.005$ ,  $\eta = 0.71$ ,  $\sigma_3 = 0.004$  and the initial variables  $S_0 = 2000$ ,  $B_0 = 1500$ ,  $V_0 = 1500$ ,  $I_0 = 100$  and  $R_0 = 10$ }.

$\sigma_1 = \sigma_2 = \sigma_3 = 0.8$ ,  $\sigma_1 = \sigma_2 = \sigma_3 = 1.2$ , and  $\sigma_1 = \sigma_2 = \sigma_3 = 2.0$ . We observe that the population of infected children decreases when  $\sigma_1$ ,  $\sigma_2$ , and  $\sigma_3$  increases from 0.5 to 2.0. Observe that when the size of sick children shrinks; however, the effect is very insignificant. As a result, the saturated constant between susceptible, breastfeeding, vaccinated, and infected has a slight effect on the dynamic behavior of the model. The effect is because  $\frac{1}{1+\sigma_1 I}$ ,  $\frac{1}{1+\sigma_2 I}$ , and  $\frac{1}{1+\sigma_3 I}$  which is the inhibitory effect from behavioral change of susceptible, breastfeeding, and vaccinated children are respectively less than 1 and as such decreases the number of the infected children. Consequently, it will be advisable to shrink contact between the infected with susceptible, breastfeeding and vaccinated to the barest minimum.

Figure 12 illustrates the dynamics of rotavirus infection (RI) without vaccination and breastfeeding interventions. The observation suggests that rotavirus is likely to remain endemic, as a significant

number of children become infected. This highlights the importance of analytical interpretations in informing strategies for controlling RI and achieving higher vaccination coverage, alongside promoting breastfeeding practices at a saturation incidence rate. Successfully vaccinating more infants, encouraging breastfeeding to provide maternal antibodies, and reducing the spread of infection through an inhibitory constant (saturation incidence rate) could potentially lead to the elimination of rotavirus from the population.

## 5.1 | Model Fitting and Validations

We collected data on Rotavirus cases in children from Ahmadu Bello University Teaching Hospital in Zaria, Nigeria [50]. To validate the computational model, we used both real and simulated data. We fitted the real data, shown in Table 3, to the

model described in Equations (2a–2e). This data, which details the number of children who tested positive for Rotavirus from September 2019 to August 2020, was gathered monthly. To simplify the comparison between the real and simulated data, we first interpolated the monthly data to a daily resolution. We then applied the model’s parameters, as outlined in Table 1, to fit the results.

From Figure 13, it is evident that the real data shows three peaks on days 6, 122, and 215, respectively. However, in our simulation data, we only observed one peak on day 12, which closely aligns with the highest (second) peak in the real data. Additionally, the simulated data intersects with the real data at the first peak. Unfortunately, we were unable to replicate the remaining peaks observed in the real data. This discrepancy may be due to several factors. First, the real data only includes children who tested positive after visiting the hospital, suggesting that other

**TABLE 3** | Positive test cases for rotavirus (September 2019–August 2020).

Month	Number of infected children in 2019	Number of infected children in 2020
January	—	7
February	—	2
March	—	4
April	—	1
May	—	2
June	—	2
July	—	2
August	—	1
September	2	—
October	6	—
November	5	—
December	21	—

infected children who did not seek medical attention might not be accounted for. Second, the model assumes a constant vaccination rate during the period from September 2019 to August 2020, which may not reflect the actual day-to-day variations in vaccination rates. Lastly, the model incorporates breastfeeding, vaccination, and a saturated incidence rate to control rotavirus infection. The inclusion of a saturated incidence rate accounts for its inhibitory effect, reducing the infection rate when the number of infected children exceeds a certain threshold.

Table 4 shows that the percentage of infected children decreases when various control methods are applied, even when the incidence rate is saturated.

From Table 5, the proposed SBVIR Biomedical model can assist in planning and implementing public health interventions related to rotavirus. For instance, the model can provide critical predictions about the spread of rotavirus, helping public health officials anticipate outbreaks and optimize resource allocation. By analyzing various scenarios, the model can enable officials to prepare effectively and direct resources like vaccines and medical supplies to areas at high risk. It also aids in refining vaccination strategies by determining the most effective timing and coverage rates to curb transmission.

Furthermore, the model can identify high-risk groups based on factors such as breastfeeding and vaccination status, allowing for targeted interventions like specialized vaccination campaigns. It supports ongoing monitoring and evaluation of intervention effectiveness, providing evidence for successful strategies. The model’s insights can influence public health policy and serve as an early warning system for emerging outbreaks, ensuring a proactive response to rotavirus challenges.

## 6 | Discussion

Further analysis on the results of the Biomedical model is presented in this section. Also, the generalized limitations and a

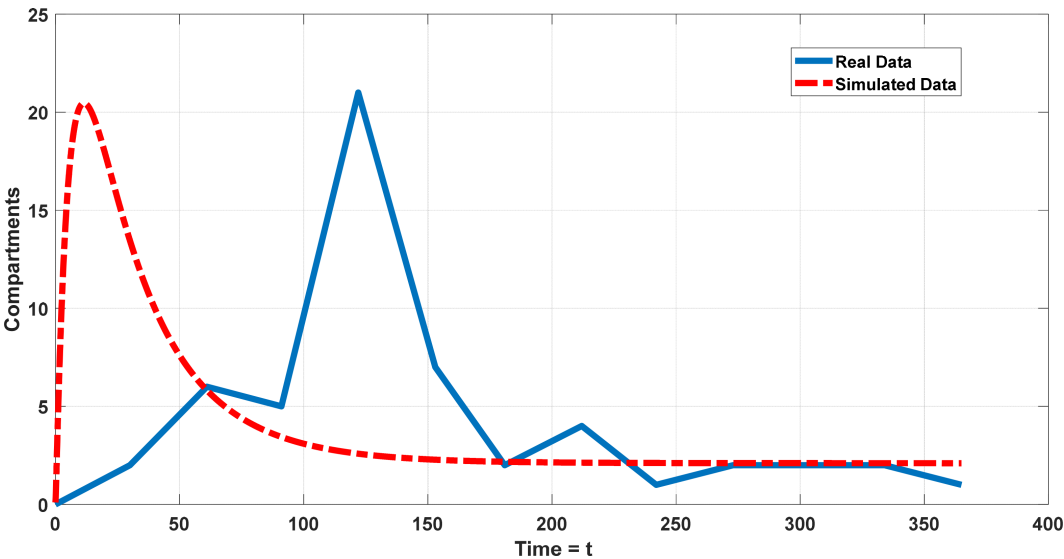


**FIGURE 13** | Computational comparison between real and simulated data.

**TABLE 4** | Percentage decrease in number of infections with different control methods under saturated incidence rate.

Control type with saturation incidence rate	Without control	With control	Percentage decrease (%)
Breastfeeding of newborn children ( $\rho$ )	63.8659	54.8528	14.1125
Vaccination of newborn children ( $\alpha$ )	63.8659	54.5234	14.6283
Breastfeeding of susceptible children ( $\Lambda$ )	63.8659	34.2081	46.4376
Vaccination of susceptible children ( $\omega$ )	63.8659	15.547	75.6568
$B$ and $V$ of newborn children ( $\rho$ and $\alpha$ )	63.8659	31.3114	50.9732
Breastfeeding and Vaccination of susceptible children ( $\Lambda$ and $\omega$ )	63.8659	32.7179	48.7709
Vaccination of breastfed children ( $\xi$ )	63.8659	54.0816	15.4140
Breastfeeding and Vaccination of newborn, susceptible, and breastfed children ( $\rho$ , $\alpha$ , $\Lambda$ , $\omega$ and $\xi$ )	2947.0953	28.7743	99.0236
Saturation Incidence Rate	89.5343	28.7743	64.5116

**TABLE 5** | Comparison of different model types with the proposed model.

Model type	SBVIR	SVIR	SBIR	SIR
Efficacy of control	99%	26%	19%	18%

practical use case for SMI are presented. Figures 2 and 3 showed the effect of  $V$  and  $B$  on the BRN of the infection while Figure 4 represents the combined effect of  $V$  and  $B$  on the BRN with  $V$  having the greatest positive effect. From Figures 5 and 6, it is seen that the susceptible children decreased, breastfed, vaccinated, infected, and recovered children oscillated before becoming constant, but a significant reduction of the infected is observed in Figure 6 because of a slight increase in the rate of breastfeeding of newborn children. This means that rotavirus can only be eradicated from the population if the control measures are effective. The performance of  $B$  and  $V$  rates to the dynamics of RI was further displayed in Figures 7 and 8. It will be observed that  $B$  and  $V$  can positively affect the dynamics of RI, that is, the more children are breastfed and vaccinated (increase in  $\rho$  and  $\alpha$ ), the fewer the children are infected with rotavirus. Figure 9 shows an increase in the number of breastfeeding and vaccinated children while the number of infected children is drastically reduced thereby increasing the recovered children from RI. Figure 10 illustrates the effect of vaccination and breastfeeding of the newborn and susceptible children on the dynamics of RI in the population from which we detected a slight increase in the parameters associated with vaccination and breastfeeding ( $\alpha$ ,  $\rho$ ,  $\omega$ ,  $\Lambda$  and  $\Lambda$ ), from which observed that RI will be eradicated. Figures 11 and 12, respectively show the effect of vaccination and breastfeeding respectively on the dynamics of the infection. The result indicated that both play a very important role in the prevention and eradication of RI in the population with vaccination having a greater effect on the dynamic of the infection.

The effect of saturated constants on the infected group was shown in Figure 13 which was plotted with  $\sigma_1 = \sigma_2 = \sigma_3 = 0.5, 0.8, .2$  and  $2.0$ . We observe that the population of infected children decreases when  $\sigma_1, \sigma_2$  and  $\sigma_3$  increases from  $0.5$  to  $2.0$ . As a result, the saturated constant between breastfeeding,

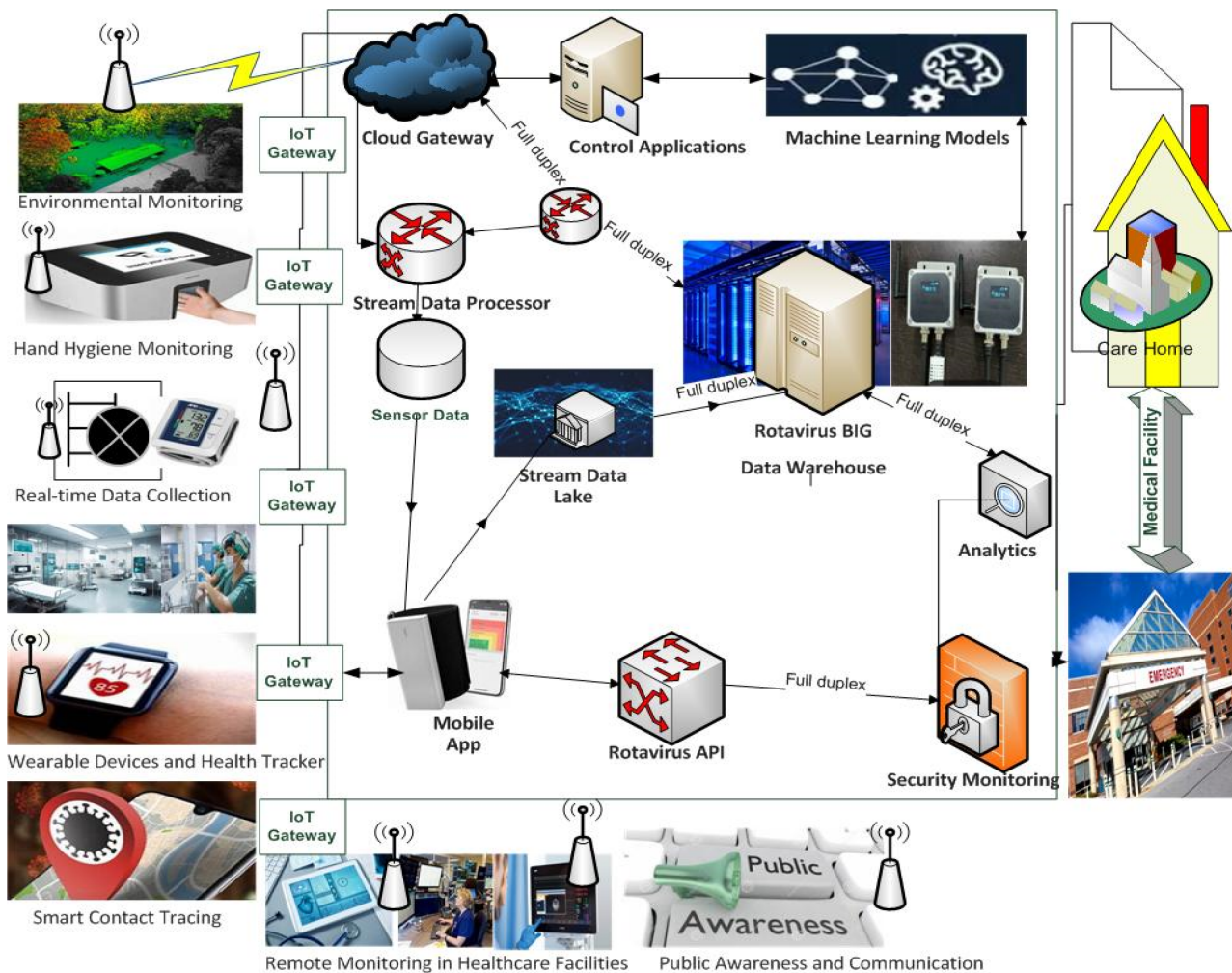
vaccinated, and infected has a slight effect on the dynamic response of the model. Consequently, it will be advisable to shrink contact between the infected and susceptible to the barest minimum.

Figure 12 shows the response of RI in the absence of  $V$  and  $B$ , from which we observed an increase in the population of the infected, and this indicates rotavirus will be endemic in the population.

It is observed from Figure A1 that the model fits well with real data to project the infected population in real life and from Table 4, that increasing vaccination and breastfeeding rates of the newborn and susceptible children together with vaccinating breastfed children, coupled with the introduction of saturation incidence, resulted in a high percentage decrease in the spread of RI and the number of infected children in the population. This is illustrated in Table 5 as we observed that the proposed model is more effective. Lastly, from numerical analysis, the proposed model recommends that effective vaccination of susceptible children and breastfeeding is sufficient to diminish the spread of RI in the population. The efficacy of breastfeeding  $B$  is elevated through encouraging mothers to breastfeed their children with the first breast milk immediately after birth and that breastfeeding should continue for up to 6 months or more (exclusive breastfeeding). Increasing access to breastfeeding education and services and promoting a positive attitude toward breastfeeding in the population can also elevate the efficacy of breastfeeding. The study indicates that efforts should be made to improve the efficiency of breastfeeding and enlarge the capacity of vaccination and inhibitory factors of the saturated incidence. The idea is to control the spread of rotavirus infection efficiently.

In Figure 14, we showcase the SHI that leverages the IoT to enable various use cases. These applications are designed to aid in managing the dynamics of rotavirus infection transmission within sampled populations. SHI with IoT enables environmental monitoring to optimize conditions that affect virus survival, ensures effective hand hygiene with sensor-equipped devices, and facilitates real-time data collection for targeted interventions. Wearable IoT devices help in the early detection of symptoms, while





**FIGURE 14** | Smart Health Infrastructure for RV disease prediction and control showcasing IoT-driven data analytics applications.

smart contact tracing tracks exposures to prevent further spread. Remote patient monitoring reduces healthcare workers' exposure risk, and IoT manages the supply chain for timely resource distribution. Additionally, IoT technologies enhance public awareness and compliance by delivering real-time information on preventive measures and outbreak alerts.

In summary, the use of Social and Health Informatics (SHI) for disease analytics represents the future of infection prevention, diagnosis, control, and intervention, particularly for communicable diseases. This model can be applied in various settings, including rural areas in developing countries, care homes, orphanages, and hospitals, as well as during epidemics and pandemics. Health systems with SHI can explore the insights provided in Figure 14, especially with the advent of digital innovations in medicine such as AI, machine learning, IoT, analytics, and telemedicine.

This study has limitations briefly discussed. For instance, the work relies on advanced models to simulate rotavirus dynamics, which are simplifications of complex real-world scenarios and may not fully capture the nuances of disease spread due to varying assumptions. The model assumes a homogeneous population, ignoring individual differences in susceptibility, behavior, and healthcare access. Additionally, uncertainties in model parameters like transmission rates or vaccine efficacy are not fully

addressed. External influences such as changes in public health policies, societal behaviors, or economic conditions are not considered, nor are variations in human behavior that impact vaccination and contact patterns. The analysis also does not explore the interactions between vaccination, breastfeeding, and disease transmission in depth, nor does it examine how sensitive the results are to changes in real-world parameters. Furthermore, the model does not account for factors like healthcare infrastructure, population mobility, and the temporal dynamics of outbreaks, such as seasonal variations and long-term trends.

## 7 | Conclusion

This paper introduces a novel computational SBVIR Biomedical model with a saturated incidence function, designed to examine the impact of breastfeeding ( $B$ ) and vaccination ( $V$ ) on disease transmission dynamics. Within the framework of Biomedical epidemiology, it was observed that reducing the Basic Reproduction Number (BRN) related to  $B$  and  $V$  to below 1 ( $BRN < 1$ ) is crucial for eradicating the disease. The study highlighted the importance of increasing the efficacy and capacity of  $B$  and  $V$  to provide sufficient protection for susceptible children. We demonstrated the global stability of the disease-free equilibrium using the Lyapunov function. Additionally, we established that

both the disease-free equilibrium and the endemic equilibrium point  $E^*$  are locally asymptotically stable when  $R_{BV} < 1$  and  $R_{BV} > 1$ , respectively. By increasing parameters associated with vaccination and breastfeeding—such as  $\rho$ ,  $\Lambda$ ,  $\alpha$ ,  $\omega$ ,  $\xi$ —to cover a larger population of newborns and susceptible infants, the spread of rotavirus infection (RI) can be significantly minimized. This implies that maintaining the BRN below unity through enhanced efforts in vaccinating and breastfeeding susceptible infants, along with managing the saturation incidence rate, can lead to the eradication of RI. Otherwise, the infection will persist endemically in the population. The study also found that increasing the saturation incidence rate, which acts as an inhibitory factor, significantly reduces the number of rotavirus-infected infants. The paper concludes that without effective control measures, rotavirus will remain endemic. It is recommended that comprehensive vaccination programs and breastfeeding practices are essential to reducing the spread of RI. Future research will focus on utilizing artificial intelligence to predict the 3D structural patterns of rotavirus spike proteins and deploying Smart Health Infrastructure for similar disease prediction.

## Author Contributions

**Titus Ifeanyi Chinebu:** conceptualization, writing – original draft, investigation. **Kennedy Chinedu Okafor:** writing – original draft, conceptualization, project administration, supervision, writing – review and editing, funding acquisition. **Omowunmi Mary Longe:** writing – review and editing, project administration, resources, supervision, methodology. **Kelvin Anoh:** visualization, formal analysis, project administration, resources, data curation, software. **Henrietta Onyinye Uzoeto:** conceptualization, methodology, validation, supervision, visualization, writing – original draft, writing – review and editing. **Victor Onukwube Apeh:** writing – original draft, investigation, validation, formal analysis, data curation, methodology. **Ijeoma Peace Okafor:** data curation, writing – review and editing, resources, visualization, methodology. **Bamidele Adebisi:** funding acquisition, project administration, supervision. **Chukwunenye Anthony Okoronkwo:** project administration, resources, supervision, validation.

## Ethics Statement

Approval from an ethics committee was deemed unnecessary for this study, and informed consent was not sought, as it did not entail animal experimentation or human behavioral studies. Instead, we conducted a thorough review of existing research and included relevant references.

## Conflicts of Interest

The authors declare no conflicts of interest.

## Data Availability Statement

The data that support the findings of this study are available on request from the corresponding author. The data are not publicly available due to privacy or ethical restrictions.

## References

1. R. M. Hartman, A. L. Cohen, S. Antoni, et al., “Risk Factors for Mortality Among Children Younger Than Age 5 Years With Severe Diarrhea in Low- and Middle-Income Countries: Findings From the World Health Organization-Coordinated Global Rotavirus and Pediatric Diarrhea Surveillance Networks,” *Clinical Infectious Diseases* 76, no. 3 (2023): e1047–e1053, <https://doi.org/10.1093/cid/ciac561>.
2. M. S. Khoo, A. H. A. Azman, N. A. S. Ismail, A. A. Wahab, and A. Ali, “Associations Between Meteorological Variation and Hospitalisations for

Rotavirus Infections in Kuala Lumpur, Malaysia,” *Heliyon* 10 (2024): 1–9, <https://doi.org/10.1016/j.heliyon.2024.e28574>.

3. WHO, Rotavirus, accessed September 2, 2022, <https://www.who.int/teams/health-product-policy-and-standards/standards-and-specifications/vaccines-quality/rotavirus>.
4. J. E. Tate, A. H. Burton, C. Boschi-Pinto, U. D. Parashar, and World Health Organization–Coordinated Global Rotavirus Surveillance Network, “Global, Regional, and National Estimates of Rotavirus Mortality in Children <5 Years of Age, 2000–2013,” *Clinical Infectious Diseases* 62, no. Suppl 2 (2016): S96–S105, <https://doi.org/10.1093/cid/civ1013>.
5. E. Faber, S. I. Tshilwane, M. van Kleef, and A. Pretorius, “Apoptosis Versus Survival of African Horse Sickness Virus Serotype 4-Infected Horse Peripheral Blood Mononuclear Cells,” *Virus Research* 307 (2022): 198609, <https://doi.org/10.1016/j.virusres.2021.198609>.
6. S. O. Soloviov, T. S. Todosiichuk, O. V. Kovaliuk, et al., “Rotaviruses and Noroviruses as Etiological Agents of Acute Intestinal Diseases of Ukrainian Children,” *International Journal of Environmental Research and Public Health* 19, no. 8 (2022): 4660, <https://doi.org/10.3390/ijerph19084660>.
7. C. A. Omatola and A. O. Olaniran, “Rotaviruses: From Pathogenesis to Disease Control-A Critical Review,” *Viruses* 14, no. 5 (2022): 875, <https://doi.org/10.3390/v14050875>.
8. [8] A. Penge-Bonig, A. Plenge-Bönig, N. Soto-Ramírez, et al., “Breastfeeding Protects Against Acute Gastroenteritis due to Rotavirus in Infants,” *European Journal of Pediatrics* 169, no. 12 (2010): 1471–1476, <https://doi.org/10.1007/s00431-010-1245-0>.
9. V. Ghoshal, R. R. Das, M. K. Nayak, S. Singh, P. Das, and N. K. Mohakud, “Climatic Parameters and Rotavirus Diarrhea Among Hospitalized Children: A Study of Eastern India,” *Frontiers in Pediatrics* 8 (2020): 573448, <https://doi.org/10.3389/fped.2020.573448>.
10. [10] A. Swamy and C. R. Achanta, “An Investigation of Gastrointestinal Infections Using Prediction Model,” in *IEEE International Conference on Computer Science and Information Technologies (ICOSNIKOM)* (IEEE, 2022), 1–9, <https://doi.org/10.1109/ICOSNIKOM56551.2022.10034880>.
11. [11] O. Oyeboade, R. Lomotey, and R. Orji, “‘I Tried to Breastfeed but...’: Exploring Factors Influencing Breastfeeding Behaviours Based on Tweets Using Machine Learning and Thematic Analysis,” *IEEE Access* 9 (2021): 61074–61089, <https://doi.org/10.1109/ACCESS.2021.3073079>.
12. A. L. Morrow, G. M. Ruiz-Palacios, M. Altaye, et al., “Human Milk Oligosaccharides Are Associated With Protection Against Diarrhea in Breast Fed Infants,” *Journal of Pediatrics* 145, no. 3 (2004): 297–303, <https://doi.org/10.1016/j.jpeds.2004.04.054>.
13. Non Communicable Disease and Mental Health Program (NMH), [www3.patrol.gov](http://www3.patrol.gov) 2022.
14. Center for Disease Control and Prevention (CDC), [www.cdc.gov](http://www.cdc.gov).
15. World Health Organization (WHO) African Region, Nigeria to Avert 50,000 Deaths in Children Annually, Introduces Rotavirus Vaccine Into Vaccination Schedule, <https://www.afro.who.int/countries/nigeria/news/nigeria-avert-50000-deaths-children-annually-introduces-rotavirus-vaccine-vaccination-schedule> 2022.
16. E. O. Asare, M. A. al-Mamun, G. E. Armah, et al., “Modeling of Rotavirus Transmission Dynamics and Impact of Vaccination in Ghana,” *Vaccine* 38, no. 31 (2020): 4820–4828, <https://doi.org/10.1016/j.vaccine.2020.05.057>.
17. S. A. Madhi, N. A. Cunliffe, D. Steele, et al., “Effect of Human Rotavirus Vaccine on Severe Diarrhea in African Infants,” *New England Journal of Medicine* 362, no. 4 (2010): 289–298, <https://doi.org/10.1056/NEJMoa0904797>.
18. C. D. Ojobor, C. V. Olovo, L. O. Onah, and A. C. Ike, “Prevalence and Associated Factors to Rotavirus Infection in Children Less Than 5 Years in

- Enugu State, Nigeria,” *Virus Disease* 31, no. 3 (2020): 316–322, <https://doi.org/10.1007/s13337-020-00614-x>.
19. A. L. Jenner, M. Smalley, D. Goldman, et al., “Agent-Based Computational Modeling of Glioblastoma Predicts That Stromal Density Is Central to Oncolytic Virus Efficacy,” *iScience* 25, no. 6 (2022): 104395, <https://doi.org/10.1016/j.isci.2022.104395>.
  20. X. Liu, E. J. Pappas, M. L. Husby, B. B. Motsa, R. V. Stahelin, and E. Pienaar, “Mechanisms of Phosphatidylserine Influence on Viral Production: A Computational Model of Ebola Virus Matrix Protein Assembly,” *Journal of Biological Chemistry* 298, no. 7 (2022): 102025, <https://doi.org/10.1016/j.jbc.2022.102025>.
  21. [21] J. Liou and H. Mani, “Computational Construction of Hepatitis C Virus Core Protein Tertiary Structure With Various Modeling Methods,” *Biophysical Journal* 122, no. 3 (2023): 181a, <https://doi.org/10.1016/j.bpj.2022.11.1122>.
  22. S. Ahmad, A. Ullah, M. Arfan, and K. Shah, “On Analysis of the Fractional Mathematical Model of Rotavirus Epidemic With the Effects of Breastfeeding and Vaccination Under Atangana-Baleanu (AB) Derivative,” *Chaos, Solitons & Fractals* 140 (2020): 110233, <https://doi.org/10.1016/j.chaos.2020.110233>.
  23. Y. D. Devi, A. Devi, H. Gogoi, et al., “Exploring Rotavirus Proteome to Identify Potential B- and T-Cell Epitope Using Computational Immunoinformatics,” *Heliyon* 6, no. 12 (2020): e05760, <https://doi.org/10.1016/j.heliyon.2020.e05760>.
  24. A. N. M. Kraay, M. K. Steele, J. M. Baker, et al., “Predicting the Long-Term Impact of Rotavirus Vaccination in 112 Countries From 2006 to 2034: A Transmission Modeling Analysis,” *Vaccine* 40, no. 46 (2022): 6631–6639, <https://doi.org/10.1016/j.vaccine.2022.09.072>.
  25. [25] J. E. Tate, A. H. Burton, C. Boschi-Pinto, et al., “2008 Estimate of Worldwide Rotavirus-Associated Mortality in Children Younger Than 5 Years Before the Introduction of Universal Rotavirus Vaccination Programmes: A Systematic Review and Meta-Analysis,” *Lancet Infectious Diseases* 12, no. 2 (2012): 136–141, [https://doi.org/10.1016/S1473-3099\(11\)70253-5](https://doi.org/10.1016/S1473-3099(11)70253-5).
  26. [26] S. E. Shuaib and P. Riyapan, “A Mathematical Model to Study the Effect of Breastfeeding and Vaccination on Rotavirus Epidemics,” *Journal of Mathematical and Fundamental Sciences* 52, no. 1 (2020): 43–65, <https://doi.org/10.5614/j.math.fund.sci.2020.52.1.4>.
  27. J. Zhang, J. Jia, and X. Song, “Analysis of an SEIR Epidemic Model With Saturated Incidence and Saturated Treatment Function,” *Scientific World Journal* 2014 (2014): 1–11.
  28. L. Esteva and M. Matias, “A Model for Vector Transmitted Diseases With Saturation Incidence,” *Journal of Biological Systems* 9, no. 4 (2001): 245–253, <https://doi.org/10.1142/S0218339001000414>.
  29. [29] O. Adebimpe, L. M. Erinle-Ibrahim, and A. F. Adebisi, “Stability Analysis of SIQS Epidemic With Saturated Incidence Rate,” *Applied Mathematics* 7 (2016): 1082–1086, <https://doi.org/10.4236/am.2016.710096>.
  30. [30] O. L. Omondi, C. Wang, X. Xue, and O. G. Lawi, “Modeling the Effects of Vaccination on Rotavirus Infection,” *Adv. Differential Equations* 2015, no. 1 (2015): 281, <https://doi.org/10.1186/s13662-015-0722-1>.
  31. [31] I. Darti, A. Suryanto, and N. B. Ilmi, “Dynamical Behavior of a Rotavirus Transmission Model With an Environmental Effects,” *AIP Conference Proceedings* 2264 (2020): 020001, <https://doi.org/10.1063/5.0023487>.
  32. [32] F. A. Adongo, O. O. Lawrence, J. Bonyo, G. O. Lawi, and O. A. Elisha, “A Delayed Vaccination Model for Rotavirus Infection,” *European Journal of Pure and Applied Mathematics* 13, no. 4 (2020): 840–851, <https://doi.org/10.29020/nybg.ejpam.v13i4.3822>.
  33. [33] P. Tharmaphornpilas, S. Jiamsiri, S. Boonchaiya, et al., “Evaluating the First Introduction of Rotavirus Vaccine in Thailand: Moving From Evidence to Policy,” *Vaccine* 35, no. 5 (2017): 796–801, <https://doi.org/10.1016/j.vaccine.2016.12.043>.
  34. [34] D. Walters, S. Horton, A. Y. Siregar, et al., “The Cost of Not Breastfeeding in Southeast Asia,” *Health Policy and Planning* 31, no. 8 (2016): 1107–1116, <https://doi.org/10.1093/heapol/czw044>.
  35. [35] B. A. Lopman, V. E. Pitzer, R. Sarkar, et al., “Understanding Reduced Rotavirus Vaccine Efficacy in Low Socio-Economic Settings,” *PLoS One* 7, no. 8 (2012): 1–7, <https://doi.org/10.1371/journal.pone.0041720>.
  36. [36] V. Jiang, B. Jiang, J. Tate, U. D. Parashar, and M. M. Patel, “Performance of Rotavirus Vaccines in Developed and Developing Countries,” *Human Vaccines & Immunotherapeutics* 6, no. 7 (2010): 532–542, <https://doi.org/10.4161/hv.6.7.11278>.
  37. [37] A. Krawczyk, M. G. Lewis, B. T. Venkatesh, and S. N. Nair, “Effect of Exclusive Breastfeeding on Rotavirus Infection Among Children,” *Indian Journal of Pediatrics* 83, no. 3 (2016): 220–225, <https://doi.org/10.1007/s12098-015-1854-8>.
  38. [38] U. D. Parashar, E. G. Hummelman, J. S. Bresee, M. A. Miller, and R. I. Glass, “Global Illness and Deaths Caused by Rotavirus Disease in Children,” *Emerging Infectious Diseases* 9, no. 5 (2003): 565–572, <https://doi.org/10.3201/eid0905.020562>.
  39. D. B. Middleton, “Rotavirus Infection: Optimal Treatment and Prevention,” *Journal of Family Practice* 60, no. 5 (2011): E1–E6, <https://doi.org/10.1542/peds.2006-3134>.
  40. [40] N. Paraz, “Rotavirus Gastroenteritis: Why to Back Up the Development of New Vaccines,” *Comparative Immunology, Microbiology and Infectious Diseases* 31, no. 2–3 (2008): 253–269, <https://doi.org/10.1016/j.cimid.2007.07.005>.
  41. G. Birkhoff and G. C. Rota, *Ordinary Differential Equations*, 4th ed. (John Wiley and Sons Inc, 1989).
  42. J. P. LaSalle, *The Stability of Dynamic Systems* (Society for Industrial and Applied Mathematics, 1976).
  43. [43] N. B. Ilmi, I. Darti, and A. Suryanto, “Dynamic Analysis of Rotavirus Infection Model With Vaccination and Saturated Incidence Rate,” *Journal of Physics: Conference Series* 1562 (2020): 012018, <https://doi.org/10.1088/1742-6596/1562/1/012018>.
  44. S. Bowong and J. Kurths, “Modelling Tuberculosis and Hepatitis b Co-Infections,” *Mathematical Modelling of Natural Phenomena* 5, no. 6 (2010): 196–242, <https://doi.org/10.1051/mmnp/20105610>.
  45. U. D. Parashar, E. A. Nelson, and G. Kang, “Diagnosis, Management, and Prevention of Rotavirus Gastroenteritis in Children,” *BMJ* 347 (2013): f7204, <https://doi.org/10.1136/bmj.f7204>.
  46. C. I. Agency, *The CIA World Factbook 2012* (Skyhorse Publishing, 2012).
  47. J. E. Tate, R. D. Rheingans, C. E. O’Reilly, et al., “Rotavirus Disease Burden and Impact and Cost-Effectiveness of a Rotavirus Vaccination Program in Kenya,” *Journal of Infectious Diseases* 200, no. Suppl. 1 (2009): 576–584, <https://doi.org/10.1086/605058>.
  48. T. Vesikari, A. Karvonen, R. Prymula, et al., “Efficacy of Human Rotavirus Vaccine Against Gastroenteritis During the First 2 Years of Life in European Infants: Randomized, Double-Blind Control Study,” *Lancet* 370 (2007): 1757–1763, [https://doi.org/10.1016/S0140-6736\(07\)61744-9](https://doi.org/10.1016/S0140-6736(07)61744-9).
  49. T. Vesikari, D. O. Matson, P. Dennehy, et al., “Safety and Efficacy of a Pentavalent Human-Bovine (WC3) Reassortant Rotavirus Vaccine,” *New England Journal of Medicine* 354 (2006): 23–33, <https://doi.org/10.1086/505151>.
  50. S. M. Mado, F. J. Giwa, S. M. Abdullahi, et al., “Prevalence and Characteristics of Rotavirus Acute Gastroenteritis Among Under-Five Children in Ahmadu Bello University Teaching Hospital, Zaria, Nigeria,” *Annals of African Medicine* 21, no. 3 (2022): 283–287, [https://doi.org/10.4103/aam.aam\\_31\\_21](https://doi.org/10.4103/aam.aam_31_21).



## Appendix A

To compute the EEP of the rotavirus epidemic model, we use system (2) and obtain.

$$\left. \begin{aligned} 0 &= (1 - \rho - \alpha)\psi + \tau B^* + \gamma V^* - \left( \frac{\beta I^*}{1 + \sigma_1 I^*} + \Lambda + \omega + \mu \right) S^* \\ 0 &= \rho\psi + \Lambda S^* - \left( \frac{\varepsilon \beta I^*}{1 + \sigma_2 I^*} + \xi + \tau + \mu \right) B^* \\ 0 &= \alpha\psi + \xi B^* + \omega S^* - \left( \frac{\eta \beta I^*}{1 + \sigma_3 I^*} + \mu + \gamma \right) V^* \\ 0 &= \frac{\beta S^* I^*}{1 + \sigma_1 I^*} + \frac{\varepsilon \beta B^* I^*}{1 + \sigma_2 I^*} + \frac{\eta \beta V^* I^*}{1 + \sigma_3 I^*} - (\phi + \theta + \mu) I^* \\ 0 &= \theta I^* - \mu R^* \end{aligned} \right\} \quad (A1)$$

From this we get

$$S^* = \frac{\left[ \begin{aligned} &\psi(1 + \sigma_1 I^*)[\varepsilon \beta I^* + (\xi + \tau + \mu)(1 + \sigma_2 I^*)][\eta \beta I^* + (\mu + \gamma)(1 + \sigma_3 I^*)] \\ &- \psi \rho \varepsilon \beta I^*(1 + \sigma_1 I^*)[\eta \beta I^* + (\mu + \gamma)(1 + \sigma_3 I^*)] - \psi \rho \xi \eta \beta I^*(1 + \sigma_1 I^*)(1 + \sigma_2 I^*) \\ &- \psi \rho \mu \eta \beta I^*(1 + \sigma_1 I^*)(1 + \sigma_2 I^*) - \psi \rho \xi \mu(1 + \sigma_1 I^*)(1 + \sigma_2 I^*)(1 + \sigma_3 I^*) \\ &- \psi \rho \mu(\mu + \gamma)(1 + \sigma_1 I^*)(1 + \sigma_2 I^*)(1 + \sigma_3 I^*) \\ &- \psi \alpha \eta \beta I^*(1 + \sigma_1 I^*)[\varepsilon \beta I^* + (\xi + \tau + \mu)(1 + \sigma_2 I^*)] \\ &- \psi \alpha \mu(1 + \sigma_1 I^*)(1 + \sigma_3 I^*)[\varepsilon \beta I^* + (\xi + \tau + \mu)(1 + \sigma_2 I^*)] \end{aligned} \right]}{(A2)}$$

$$\left[ \begin{aligned} &\beta I^*[\varepsilon \beta I^* + (\xi + \tau + \mu)(1 + \sigma_2 I^*)][\eta \beta I^* + (\mu + \gamma)(1 + \sigma_3 I^*)] \\ &+ \Lambda \varepsilon \beta I^*(1 + \sigma_1 I^*)[\eta \beta I^* + (\mu + \gamma)(1 + \sigma_3 I^*)] \\ &+ \Lambda \xi \eta \beta I^*(1 + \sigma_1 I^*)(1 + \sigma_2 I^*) \\ &+ \Lambda \xi \mu(1 + \sigma_1 I^*)(1 + \sigma_2 I^*)(1 + \sigma_3 I^*) \\ &+ \Lambda \mu(1 + \sigma_1 I^*)(1 + \sigma_2 I^*)[\eta \beta I^* + (\mu + \gamma)(1 + \sigma_3 I^*)] \\ &+ \omega \eta \beta I^*(1 + \sigma_1 I^*)[\varepsilon \beta I^* + (\xi + \tau + \mu)(1 + \sigma_2 I^*)] \\ &+ \omega \mu(1 + \sigma_1 I^*)(1 + \sigma_3 I^*)[\varepsilon \beta I^* + (\xi + \tau + \mu)(1 + \sigma_2 I^*)] \\ &+ \mu \eta \beta I^*(1 + \sigma_1 I^*)[\varepsilon \beta I^* + (\xi + \tau + \mu)(1 + \sigma_2 I^*)] \\ &+ \mu(\mu + \gamma)(1 + \sigma_1 I^*)(1 + \sigma_3 I^*)[\varepsilon \beta I^* + (\xi + \tau + \mu)(1 + \sigma_2 I^*)] \end{aligned} \right]$$

$$\left[ \begin{aligned} &\rho \psi \beta I^*(1 + \sigma_2 I^*)[\eta \beta I^* + (\mu + \gamma)(1 + \sigma_3 I^*)] + \rho \psi \omega \eta \beta I^*(1 + \sigma_1 I^*)(1 + \sigma_2 I^*) \\ &+ \rho \psi \omega \mu(1 + \sigma_1 I^*)(1 + \sigma_2 I^*)(1 + \sigma_3 I^*) + \rho \psi \mu \eta \beta I^*(1 + \sigma_1 I^*)(1 + \sigma_2 I^*) \\ &+ \rho \psi \mu(\mu + \gamma)(1 + \sigma_1 I^*)(1 + \sigma_2 I^*)(1 + \sigma_3 I^*) \\ &+ \Lambda \psi(1 + \sigma_1 I^*)(1 + \sigma_2 I^*)[\eta \beta I^* + (\mu + \gamma)(1 + \sigma_3 I^*)] \\ &- \Lambda \psi \alpha \eta \beta I^*(1 + \sigma_1 I^*)(1 + \sigma_2 I^*) - \Lambda \psi \alpha \mu(1 + \sigma_1 I^*)(1 + \sigma_2 I^*)(1 + \sigma_3 I^*) \end{aligned} \right] \quad (A3)$$



$$V^* = \frac{\begin{bmatrix} \alpha\psi\beta I^*(1+\sigma_3 I^*)[\varepsilon\beta I^* + (\xi + \tau + \mu)(1+\sigma_2 I^*)] \\ +\alpha\psi\Lambda\varepsilon\beta I^*(1+\sigma_1 I^*)(1+\sigma_3 I^*) \\ +\alpha\psi\Lambda\mu(1+\sigma_1 I^*)(1+\sigma_2 I^*)(1+\sigma_3 I^*) \\ +\alpha\psi\mu(1+\sigma_1 I^*)(1+\sigma_3 I^*)[\varepsilon\beta I^* + (\xi + \tau + \mu)(1+\sigma_2 I^*)] \\ +\xi\rho\psi\beta I^*(1+\sigma_2 I^*)(1+\sigma_3 I^*) \\ +\xi\rho\psi\mu(1+\sigma_1 I^*)(1+\sigma_2 I^*)(1+\sigma_3 I^*) \\ +\xi\Lambda\psi(1+\sigma_1 I^*)(1+\sigma_2 I^*)(1+\sigma_3 I^*) \\ +\omega\psi(1+\sigma_1 I^*)(1+\sigma_3 I^*)[\varepsilon\beta I^* + (\xi + \tau + \mu)(1+\sigma_2 I^*)] \\ -\omega\psi\rho\varepsilon\beta I^*(1+\sigma_1 I^*)(1+\sigma_3 I^*) \\ -\omega\psi\rho\mu(1+\sigma_1 I^*)(1+\sigma_2 I^*)(1+\sigma_3 I^*) \end{bmatrix}}{\begin{bmatrix} \beta I^*[\varepsilon\beta I^* + (\xi + \tau + \mu)(1+\sigma_2 I^*)][\eta\beta I^* + (\mu + \gamma)(1+\sigma_3 I^*)] \\ +\Lambda\varepsilon\beta I^*(1+\sigma_1 I^*)[\eta\beta I^* + (\mu + \gamma)(1+\sigma_3 I^*)] \\ +\Lambda\xi\eta\beta I^*(1+\sigma_1 I^*)(1+\sigma_2 I^*) \\ +\Lambda\xi\mu(1+\sigma_1 I^*)(1+\sigma_2 I^*)(1+\sigma_3 I^*) \\ +\Lambda\mu(1+\sigma_1 I^*)(1+\sigma_2 I^*)[\eta\beta I^* + (\mu + \gamma)(1+\sigma_3 I^*)] \\ +\omega\eta\beta I^*(1+\sigma_1 I^*)[\varepsilon\beta I^* + (\xi + \tau + \mu)(1+\sigma_2 I^*)] \\ +\omega\mu(1+\sigma_1 I^*)(1+\sigma_3 I^*)[\varepsilon\beta I^* + (\xi + \tau + \mu)(1+\sigma_2 I^*)] \\ +\mu\eta\beta I^*(1+\sigma_1 I^*)[\varepsilon\beta I^* + (\xi + \tau + \mu)(1+\sigma_2 I^*)] \\ +\mu(\mu + \gamma)(1+\sigma_1 I^*)(1+\sigma_3 I^*)[\varepsilon\beta I^* + (\xi + \tau + \mu)(1+\sigma_2 I^*)] \end{bmatrix}} \quad (\text{A4})$$

$$R^* = \frac{\theta I^*}{\mu} \quad (\text{A5})$$

and

$$\begin{aligned} & \left[ (\phi + \theta + \mu) \begin{pmatrix} \varepsilon\eta\beta^3 + \varepsilon\beta^2\sigma_3(\mu + \gamma) + \beta\sigma_2\sigma_3(\xi + \tau + \mu)(\mu + \gamma) + \Lambda\eta\beta^2\sigma_1 + \Lambda\varepsilon\beta\sigma_2\sigma_3(\mu + \gamma) \\ +\Lambda\varepsilon\eta\beta\sigma_1\sigma_2 + \Lambda\xi\mu\sigma_1\sigma_2\sigma_3 + \Lambda\mu\eta\beta\sigma_1\sigma_2 + \Lambda\mu\sigma_1\sigma_2\sigma_3(\mu + \gamma) + \omega\eta\varepsilon\beta\sigma_1 \\ +\omega\eta\beta\sigma_1\sigma_2(\xi + \tau + \mu) + \omega\mu\varepsilon\beta\sigma_1\sigma_3 + \omega\mu\sigma_1\sigma_2\sigma_3(\xi + \tau + \mu) + \mu\eta\varepsilon\beta^2\sigma_1 \\ +\mu\eta\beta\sigma_1\sigma_2(\xi + \tau + \mu) + \varepsilon\mu\beta\sigma_1\sigma_3(\mu + \gamma) + \mu\sigma_1\sigma_2\sigma_3(\xi + \tau + \mu)(\mu + \gamma) \end{pmatrix} \right] I^{*3} \\ & + \left[ (\phi + \theta + \mu) \begin{pmatrix} \varepsilon\beta^2(\mu + \gamma) + \eta\beta^2(\xi + \tau + \mu) + \beta\sigma_3(\xi + \tau + \mu)(\mu + \gamma) + \eta\beta^2\sigma_2(\xi + \tau + \mu) \\ +\beta\sigma_2(\xi + \tau + \mu) + \Lambda\varepsilon\eta\beta^2 + \Lambda\varepsilon\beta\sigma_3 + \Lambda\varepsilon\beta\sigma_1(\mu + \gamma) + \Lambda\varepsilon\eta\beta(\sigma_1 + \sigma_2) \\ +\Lambda\xi\mu(\sigma_1\sigma_2 + \sigma_2\sigma_3 + \sigma_1\sigma_3) + \Lambda\mu\eta\beta(\sigma_1 + \sigma_2) + \Lambda\mu(\mu + \gamma)(\sigma_1\sigma_3 + \sigma_2\sigma_3) \\ +\Lambda\mu\sigma_1\sigma_2(\mu + \gamma) + \omega\eta\varepsilon\beta^2 + \omega\eta\beta\sigma_2(\xi + \tau + \mu) + \omega\eta\beta\sigma_1(\xi + \tau + \mu) + \mu\eta\varepsilon\beta^2 \\ +\omega\mu\varepsilon\beta(\sigma_1 + \sigma_3) + \omega\mu(\xi + \tau + \mu)(\sigma_1\sigma_2 + \sigma_2\sigma_3) + \omega\mu\sigma_1\sigma_3(\xi + \tau + \mu) \\ +\mu\eta\beta\sigma_2(\xi + \tau + \mu) + \mu\eta\beta\sigma_1(\xi + \tau + \mu) + \varepsilon\mu\beta(\mu + \gamma)(\sigma_1 + \sigma_3) \\ +\mu(\xi + \tau + \mu)(\mu + \gamma)(\sigma_1\sigma_2 + \sigma_2\sigma_3) + \mu\sigma_1\sigma_3(\xi + \tau + \mu)(\mu + \gamma) \end{pmatrix} \right] I^{*2} \\ & - \varepsilon\eta\psi\beta^3 - \psi\beta^2\sigma_3(\mu + \gamma) - \eta\psi\beta^2\sigma_2(\xi + \tau + \mu) - \psi\beta\sigma_2(\xi + \tau + \mu)(\mu + \gamma) + \xi\rho\eta\psi\beta^2\sigma_2 \\ & + \mu\xi\rho\psi\beta\sigma_2\sigma_3 + \mu\rho\psi\eta\beta^2\sigma_2 + \mu\rho\psi\beta\sigma_2\sigma_3(\mu + \gamma) + \psi\rho\varepsilon\eta\beta^3 + \psi\rho\varepsilon\beta^2\sigma_3 + \psi\alpha\varepsilon\eta\beta^3 \\ & + \psi\alpha\eta\beta^2\sigma_2(\xi + \tau + \mu) + \psi\alpha\mu\varepsilon\beta^2\sigma_3 + \psi\alpha\mu\beta\sigma_2\sigma_3(\xi + \tau + \mu) - \psi\rho\varepsilon\eta\beta^3 - \psi\rho\varepsilon\beta^2\sigma_3(\mu + \gamma) \\ & - \psi\rho\varepsilon\eta\beta^2\sigma_1 - \psi\rho\varepsilon\omega\mu\beta\sigma_1\sigma_2 - \psi\rho\varepsilon\mu\eta\beta^2\sigma_1 - \Lambda\psi\varepsilon\eta\beta^2\sigma_1 - \Lambda\psi\varepsilon\beta\sigma_1\sigma_3(\mu + \gamma) + \Lambda\psi\alpha\varepsilon\eta\beta^2\sigma_1 \\ & + \Lambda\mu\psi\alpha\varepsilon\beta\sigma_1\sigma_3 - \alpha\psi\varepsilon\eta\beta^3 - \alpha\psi\eta\beta^2(\xi + \tau + \mu) - \Lambda\psi\alpha\varepsilon\beta^2\sigma_1 - \Lambda\mu\psi\alpha\eta\beta\sigma_1\sigma_2 - \mu\psi\alpha\eta\varepsilon\beta^2\sigma_1 \\ & - \mu\psi\alpha\eta\beta\sigma_1\sigma_2(\xi + \tau + \mu) - \xi\psi\eta\beta^2\sigma_2 - \xi\rho\psi\mu\eta\beta\sigma_1\sigma_2 - \xi\Lambda\psi\eta\beta\sigma_1\sigma_2 - \omega\psi\eta\varepsilon\beta^2\sigma_1 \\ & - \omega\psi\eta\beta\sigma_1\sigma_2(\xi + \tau + \mu) + \omega\psi\rho\mu\eta\beta\sigma_1\sigma_2 + \omega\psi\rho\varepsilon\eta\beta^2\sigma_1 \end{aligned} \\ & + \left[ (\phi + \theta + \mu) \begin{pmatrix} \beta(\xi + \tau + \mu)(\mu + \gamma) + \Lambda\varepsilon\beta(\mu + \gamma) + \Lambda\varepsilon\eta\beta + \Lambda\xi\mu(\sigma_1 + \sigma_2 + \sigma_3) + \Lambda\mu\eta\beta \\ +\Lambda\mu(\mu + \gamma) + \Lambda\mu(\mu + \gamma)(\sigma_1 + \sigma_3) + \omega\eta\beta(\xi + \tau + \mu) + \omega\mu\varepsilon\beta \\ +\omega\mu\sigma_2(\xi + \tau + \mu) + \omega\mu(\xi + \tau + \mu)(\sigma_1 + \sigma_3) + \mu\eta\beta(\xi + \tau + \mu) \\ +\varepsilon\mu\beta(\mu + \gamma) + \mu\sigma_2(\xi + \tau + \mu)(\mu + \gamma) + \mu\sigma_2(\xi + \tau + \mu)(\mu + \gamma) \end{pmatrix} \right] I^* \\ & - \varepsilon\psi\beta^2(\mu + \gamma) - \eta\psi\beta^2(\xi + \tau + \mu) - \psi\beta(\xi + \tau + \mu)(\mu + \gamma) - \psi\beta\sigma_2(\xi + \tau + \mu)(\mu + \gamma) \\ & + \xi\rho\eta\psi\beta^2 + \mu\xi\rho\psi\beta(\sigma_2 + \sigma_3) + \mu\rho\psi\eta\beta^2 + \mu\rho\psi\beta(\mu + \gamma)(\sigma_2 + \sigma_3) + \psi\rho\varepsilon\beta(\mu + \gamma) \\ & + \psi\alpha\eta\beta^2(\xi + \tau + \mu) + \psi\alpha\mu\varepsilon\beta^2 + \psi\alpha\mu\beta\sigma_2(\xi + \tau + \mu) + \psi\alpha\mu\beta\sigma_3(\xi + \tau + \mu) \\ & - \psi\rho\varepsilon\beta^2(\mu + \gamma) - \psi\rho\varepsilon\eta\beta^2 - \psi\rho\varepsilon\omega\mu\beta(\sigma_1 + \sigma_3) - \psi\rho\varepsilon\mu\eta\beta^2 - \psi\rho\varepsilon\mu\beta\sigma_1(\mu + \gamma) \\ & - \Lambda\psi\varepsilon\eta\beta^2 - \Lambda\psi\varepsilon\beta\sigma_3(\mu + \gamma) - \Lambda\psi\varepsilon\beta\sigma_1(\mu + \gamma) + \Lambda\psi\alpha\varepsilon\eta\beta^2 + \Lambda\psi\mu\alpha\varepsilon\beta(\sigma_1 + \sigma_3) \\ & - \alpha\psi\eta\beta^2(\xi + \tau + \mu) - \Lambda\psi\alpha\varepsilon\beta^2 - \Lambda\mu\psi\alpha\eta\beta(\sigma_1 + \sigma_2) - \mu\psi\varepsilon\beta^2 - \mu\psi\alpha\eta\beta\sigma_2(\xi + \tau + \mu) \\ & - \mu\psi\alpha\eta\beta\sigma_1(\xi + \tau + \mu) - \xi\psi\eta\beta^2 - \xi\rho\psi\mu\eta\beta(\sigma_1 + \sigma_2) - \xi\Lambda\psi\eta\beta(\sigma_1 + \sigma_2) - \omega\psi\eta\varepsilon\beta^2 \\ & - \omega\psi\eta\beta(\xi + \tau + \mu) - \omega\psi\eta\beta\sigma_1(\xi + \tau + \mu) + \omega\psi\rho\mu\eta\beta(\sigma_1 + \sigma_2) + \omega\psi\rho\varepsilon\eta\beta^2 \end{aligned}$$

$$+ \left[ \begin{array}{c} (\phi + \theta + \mu)(\Lambda\xi\mu + \Lambda\mu(\mu + \gamma) + \omega\mu(\xi + \tau + \mu) + \mu(\xi + \tau + \mu)(\mu + \gamma)) \\ - \psi\beta(\xi + \tau + \mu)(\mu + \gamma) + \mu\xi\rho\psi\beta + \psi\rho\mu\beta(\mu + \gamma) + \psi\alpha\mu\beta(\xi + \tau + \mu) - \psi\rho\epsilon\omega\mu\beta \\ - \psi\rho\epsilon\mu\beta(\mu + \gamma) - \Lambda\psi\epsilon\beta(\mu + \gamma) + \Lambda\psi\mu\alpha\epsilon\beta - \Lambda\mu\psi\alpha\eta\beta - \mu\psi\alpha\eta\beta(\xi + \tau + \mu) - \xi\rho\psi\mu\eta \\ \beta - \xi\Lambda\psi\eta\beta - \omega\psi\eta\beta(\xi + \tau + \mu) + \omega\psi\rho\mu\eta\beta \end{array} \right] = 0 \quad (\text{A6})$$

## Appendix B

$$\begin{aligned} & \lambda^4 + \left[ (R_{BV} - 1)(\phi + \theta + \mu) + \left( \Lambda + \omega + \mu + \frac{\beta I^*}{1 + \sigma_1 I^*} \right) + \left( \xi + \tau + \mu + \frac{\epsilon \beta I^*}{1 + \sigma_2 I^*} \right) + \left( \mu + \gamma + \frac{\eta \beta I^*}{1 + \sigma_3 I^*} \right) \right] \lambda^3 \\ & + \left[ (R_{BV} - 1)(\phi + \theta + \mu) \left( \left( \Lambda + \omega + \mu + \frac{\beta I^*}{1 + \sigma_1 I^*} \right) + \left( \xi + \tau + \mu + \frac{\epsilon \beta I^*}{1 + \sigma_2 I^*} \right) + \left( \mu + \gamma + \frac{\eta \beta I^*}{1 + \sigma_3 I^*} \right) \right) \right. \\ & + \left( \omega + \mu + \frac{\beta I^*}{1 + \sigma_1 I^*} \right) \left( \xi + \tau + \mu + \frac{\epsilon \beta I^*}{1 + \sigma_2 I^*} \right) + \Lambda \left( \xi + \mu + \frac{\epsilon \beta I^*}{1 + \sigma_2 I^*} \right) + \left( \Lambda + \mu + \frac{\beta I^*}{1 + \sigma_1 I^*} \right) \left( \mu + \gamma + \frac{\eta \beta I^*}{1 + \sigma_3 I^*} \right) + \omega \left( \mu + \frac{\eta \beta I^*}{1 + \sigma_3 I^*} \right) \\ & \left. + \left( \xi + \tau + \mu + \frac{\epsilon \beta I^*}{1 + \sigma_2 I^*} \right) \left( \mu + \gamma + \frac{\eta \beta I^*}{1 + \sigma_3 I^*} \right) + \frac{\eta^2 \beta^2 V^* I^*}{(1 + \sigma_3 I^*)^3} \lambda^2 + \left( \frac{\beta^2 S^* I^*}{(1 + \sigma_1 I^*)^3} \right) \right] \lambda^2 \\ & + \left[ (R_{BV} - 1)(\phi + \theta + \mu) \left( \left( \Lambda + \omega + \mu + \frac{\beta I^*}{1 + \sigma_1 I^*} \right) \left( \xi + \tau + \mu + \frac{\epsilon \beta I^*}{1 + \sigma_2 I^*} \right) + \left( \mu + \gamma + \frac{\eta \beta I^*}{1 + \sigma_3 I^*} \right) \left( \Lambda + \omega + \mu + \frac{\beta I^*}{1 + \sigma_1 I^*} \right) \right. \right. \\ & + \left( \mu + \gamma + \frac{\eta \beta I^*}{1 + \sigma_3 I^*} \right) \left( \xi + \tau + \mu + \frac{\epsilon \beta I^*}{1 + \sigma_2 I^*} \right) + \tau \Lambda + \omega \gamma \left. \right) + \Lambda \xi \left( \mu + \frac{\eta \beta I^*}{1 + \sigma_3 I^*} \right) + \left( \mu + \frac{\beta I^*}{1 + \sigma_1 I^*} \right) \left( \xi + \tau + \mu + \frac{\epsilon \beta I^*}{1 + \sigma_2 I^*} \right) \left( \mu + \gamma + \frac{\eta \beta I^*}{1 + \sigma_3 I^*} \right) \\ & + \omega \left( \xi + \tau + \mu + \frac{\epsilon \beta I^*}{1 + \sigma_2 I^*} \right) \left( \mu + \frac{\eta \beta I^*}{1 + \sigma_3 I^*} \right) + \Lambda \left( \mu + \frac{\epsilon \beta I^*}{1 + \sigma_2 I^*} \right) \left( \mu + \gamma + \frac{\eta \beta I^*}{1 + \sigma_3 I^*} \right) + \left( \Lambda + \omega + \mu + \frac{\beta I^*}{1 + \sigma_1 I^*} \right) \left( \frac{\epsilon^2 \beta^2 B^* I^*}{(1 + \sigma_2 I^*)^3} \right) \\ & + \left( \frac{\xi \eta \epsilon \beta^2 B^* I^*}{(1 + \sigma_2 I^*)^2 (1 + \sigma_3 I^*)} \right) + \left( \mu + \gamma + \frac{\eta \beta I^*}{1 + \sigma_3 I^*} \right) \left( \frac{\epsilon^2 \beta^2 B^* I^*}{(1 + \sigma_2 I^*)^3} \right) + \frac{\gamma \eta \beta^2 V^* I^*}{(1 + \sigma_1 I^*) (1 + \sigma_3 I^*)^2} + \frac{\Lambda \epsilon \beta^2 S^* I^*}{(1 + \sigma_2 I^*) (1 + \sigma_1 I^*)^2} \\ & + \left( \xi + \tau + \mu + \frac{\epsilon \beta I^*}{1 + \sigma_2 I^*} \right) \left( \frac{\beta^2 S^* I^*}{(1 + \sigma_1 I^*)^3} \right) \lambda + \frac{\omega \eta \beta^2 S^* I^*}{(1 + \sigma_1 I^*)^2 (1 + \sigma_3 I^*)} + \left( \mu + \gamma + \frac{\eta \beta I^*}{1 + \sigma_3 I^*} \right) \left( \frac{\beta^2 S^* I^*}{(1 + \sigma_1 I^*)^3} \right) \left. \right] \lambda \\ & + \left[ (R_{BV} - 1)(\phi + \theta + \mu) \left( \mu + \gamma + \frac{\eta \beta I^*}{1 + \sigma_3 I^*} \right) \left( \left( \Lambda + \omega + \mu + \frac{\beta I^*}{1 + \sigma_1 I^*} \right) \left( \xi + \tau + \mu + \frac{\epsilon \beta I^*}{1 + \sigma_2 I^*} \right) \right. \right. \\ & + \left( \mu + \gamma + \frac{\eta \beta I^*}{1 + \sigma_3 I^*} \right) \tau \Lambda + \left( \xi + \tau + \mu + \frac{\epsilon \beta I^*}{1 + \sigma_2 I^*} \right) \omega \gamma + \xi \gamma \Lambda \left. \right) + \left( \omega + \mu + \frac{\beta I^*}{1 + \sigma_1 I^*} \right) \left( \xi + \tau + \mu + \frac{\epsilon \beta I^*}{1 + \sigma_2 I^*} \right) \left( \frac{\eta^2 \beta^2 V^* I^*}{(1 + \sigma_3 I^*)^3} \right) \\ & + \Lambda \left( \xi + \mu + \frac{\epsilon \beta I^*}{1 + \sigma_2 I^*} \right) \left( \frac{\eta^2 \beta^2 V^* I^*}{(1 + \sigma_3 I^*)^3} \right) + \left( \Lambda + \omega + \mu + \frac{\beta I^*}{1 + \sigma_1 I^*} \right) \left( \frac{\eta^2 \beta^2 V^* I^*}{(1 + \sigma_3 I^*)^3} \right) + \left( \xi + \tau + \mu + \frac{\epsilon \beta I^*}{1 + \sigma_2 I^*} \right) \left( \frac{\eta^2 \beta^2 V^* I^*}{(1 + \sigma_3 I^*)^3} \right) \\ & + \left( \Lambda + \omega + \mu + \frac{\beta I^*}{1 + \sigma_1 I^*} \right) \left( \frac{\xi \eta \epsilon \beta^2 B^* I^*}{(1 + \sigma_2 I^*)^2 (1 + \sigma_3 I^*)} \right) + \left( \Lambda + \mu + \frac{\beta I^*}{1 + \sigma_1 I^*} \right) \left( \mu + \gamma + \frac{\eta \beta I^*}{1 + \sigma_3 I^*} \right) \left( \frac{\epsilon^2 \beta^2 B^* I^*}{(1 + \sigma_2 I^*)^3} \right) \\ & + \omega \left( \mu + \frac{\eta \beta I^*}{1 + \sigma_3 I^*} \right) \left( \frac{\epsilon^2 \beta^2 B^* I^*}{(1 + \sigma_2 I^*)^3} \right) + \left( \frac{\epsilon^2 \beta^2 B^* I^*}{(1 + \sigma_2 I^*)^3} \right) + \frac{\tau \omega \eta \epsilon \beta^2 B^* I^*}{(1 + \sigma_3 I^*) (1 + \sigma_2 I^*)^2} + \left( \mu + \gamma + \frac{\eta \beta I^*}{1 + \sigma_3 I^*} \right) \frac{\tau \epsilon \beta^2 B^* I^*}{(1 + \sigma_1 I^*) (1 + \sigma_2 I^*)^2} \\ & + \frac{\tau \epsilon \beta^2 B^* I^*}{(1 + \sigma_1 I^*) (1 + \sigma_2 I^*)^2} + \frac{\gamma \Lambda \epsilon \eta \beta^2 V^* I^*}{(1 + \sigma_2 I^*) (1 + \sigma_3 I^*)^2} + \left( \xi + \tau + \mu + \frac{\epsilon \beta I^*}{1 + \sigma_2 I^*} \right) \frac{\gamma \eta \beta^2 V^* I^*}{(1 + \sigma_1 I^*) (1 + \sigma_3 I^*)^2} + \frac{\xi \gamma \epsilon \beta^2 B^* I^*}{(1 + \sigma_1 I^*) (1 + \sigma_2 I^*)^2} \\ & + \frac{\Lambda \xi \eta \beta I^* S^*}{(1 + \sigma_3 I^*) (1 + \sigma_1 I^*)^2} + \left( \mu + \gamma + \frac{\eta \beta I^*}{1 + \sigma_3 I^*} \right) \frac{\Lambda \epsilon \beta^2 S^* I^*}{(1 + \sigma_2 I^*) (1 + \sigma_1 I^*)^2} + \left( \xi + \tau + \mu + \frac{\epsilon \beta I^*}{1 + \sigma_2 I^*} \right) \frac{\omega \eta \beta^2 S^* I^*}{(1 + \sigma_1 I^*)^2 (1 + \sigma_3 I^*)} \\ & + \left( \xi + \tau + \mu + \frac{\epsilon \beta I^*}{1 + \sigma_2 I^*} \right) \left( \mu + \gamma + \frac{\eta \beta I^*}{1 + \sigma_3 I^*} \right) \left( \frac{\beta^2 S^* I^*}{(1 + \sigma_1 I^*)^3} \right) \left. \right] = 0 \end{aligned}$$

where the characteristic equation of system (19) at  $E^*$  is given as

Figures A1 and A2 depict the individual impacts of variables  $V$  and  $B$  on the Basic Reproduction Number (BRN) of the infection, respectively. It is noteworthy that in Figures A1–A3, the BRN values consistently remain below one. This observation indicates a reduction in the BRN, indicating a decline in the rate at which an infected child transmits the rotavirus infection within the population.

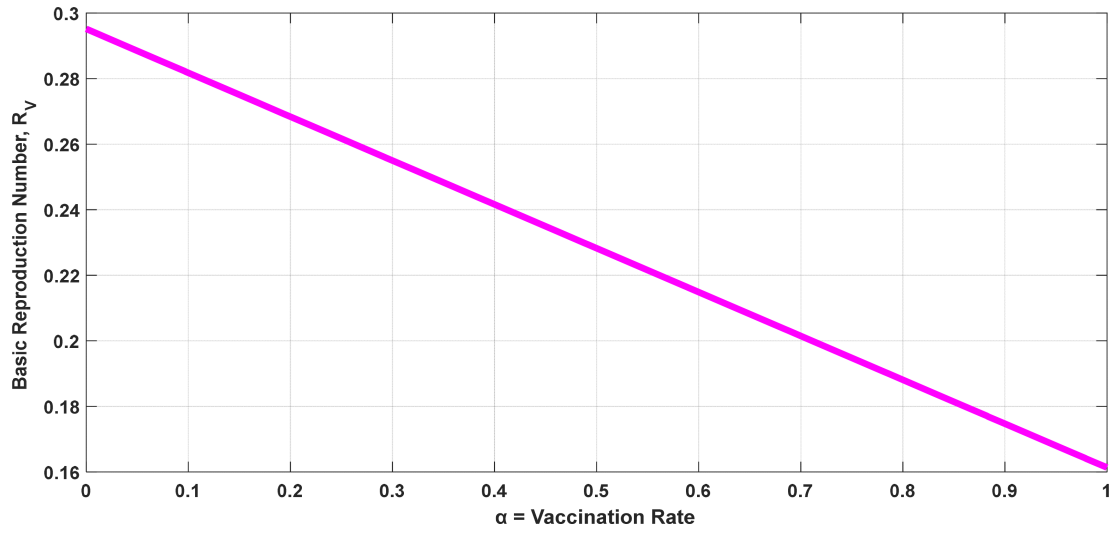


**FIGURE A1** | Numerical simulation of the basic reproduction number in the presence of  $B$  and  $V$  with parameter values  $\psi = 13.6986$ ,  $\rho = 0.00188$ ,  $\tau = 0.054945$ ,  $\gamma = 0.002778$ ,  $\xi = 0.002$ ,  $\theta = 0.8333$ ,  $\phi = 0.04466$ ,  $\Lambda = 0.22756$ ,  $\omega = 0.038191$ ,  $\beta = 0.0072$ ,  $\varepsilon = 0.00062$ ,  $\eta = 0.00071$ ,  $\mu = 0.036529$  and  $\alpha$  ranging from 0 to 1.

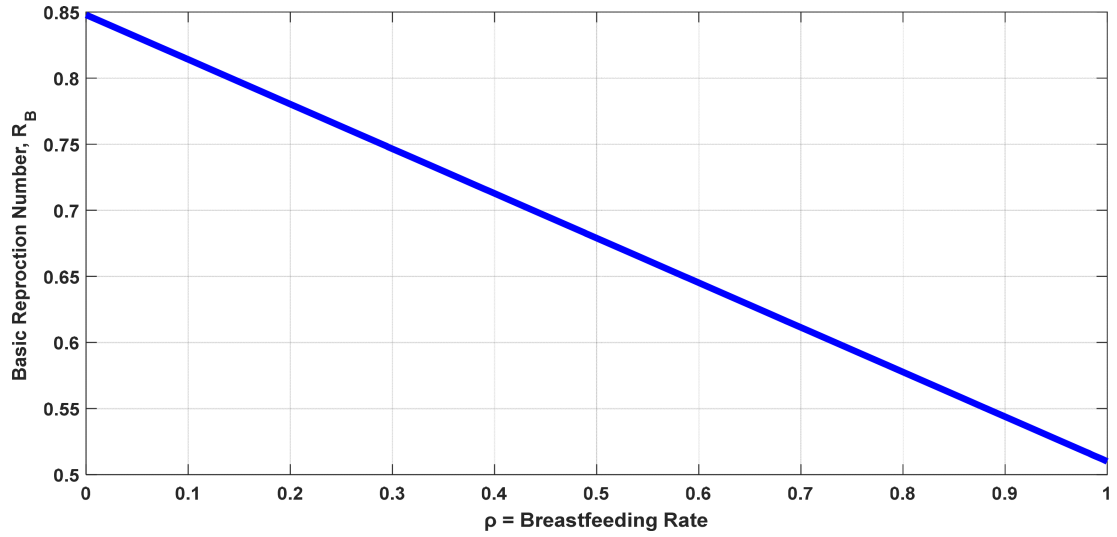


**FIGURE A2** | Numerical simulation of the basic reproduction number in the presence of  $B$  and  $V$  with parameter values  $\psi = 13.6986$ ,  $\rho = 0.00188$ ,  $\tau = 0.054945$ ,  $\gamma = 0.002778$ ,  $\xi = 0.002$ ,  $\theta = 0.8333$ ,  $\phi = 0.04466$ ,  $\Lambda = 0.22756$ ,  $\omega = 0.038191$ ,  $\beta = 0.0072$ ,  $\varepsilon = 0.00062$ ,  $\eta = 0.00071$ ,  $\mu = 0.036529$  and  $\alpha$  ranging from 0 to 1.

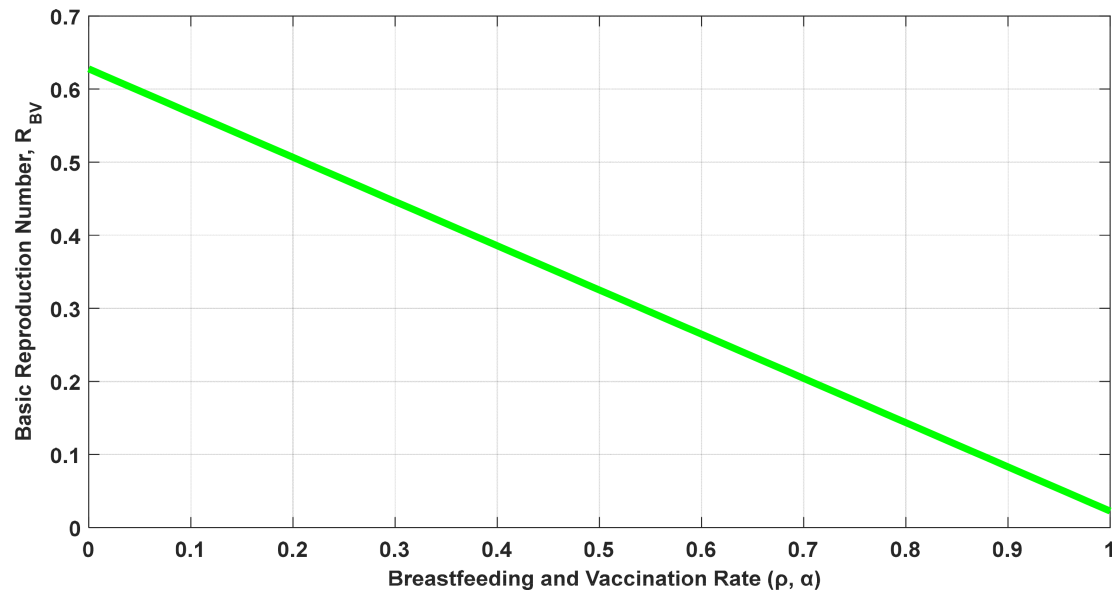


**FIGURE A3** | Numerical simulation of the basic reproduction number in the presence of  $B$  and  $V$  with parameter values  $\psi = 13.6986$ ,  $\tau = 0.054945$ ,  $\gamma = 0.002778$ ,  $\xi = 0.002$ ,  $\theta = 0.8333$ ,  $\phi = 0.04466$ ,  $\Lambda = 0.22756$ ,  $\omega = 0.038191$ ,  $\beta = 0.0072$ ,  $\varepsilon = 0.00062$ ,  $\eta = 0.00071$ ,  $\mu = 0.036529$  while  $\alpha$  and  $\rho$  respectively ranges from 0 to 1.